INDUCTION OF THE ANTIGEN PRESENTATON MACHINERY USING NOVEL SMALL MOLECULES

by

Samantha Ellis

B.Sc., University of Victoria, 2014

A THESIS SUBMITTED IN PARTIAL FULFILLMENT OF
THE REQUIRMENTS FOR THE DEGREE OF

MASTER OF SCIENCE

in

The Faculty of Graduate and Postdoctoral Studies

(Medical Genetics)

THE UNIVERSITY OF BRITISH COLUMBIA
(Vancouver)

January 2017

Abstract

The immune system is crucial in the prevention and eradication of cancer. However, cancer genomes mutate more frequently than healthy cells and a commonly acquired phenotype is reduced expression of the antigen presentation machinery (APM) that is required for immunosurveillance. This phenotype can allow cancer cells to become invisible to the immune system and metastasize with limited inhibition. Since this phenomenon is seen across a wide variety of cancers discovering methods to reverse this immune evasion could lead to the development of widely applicable therapeutics.

A compound, S-(+)-curcuphenol was previously identified as a novel candidate for restoring expression of the APM, however, its synthesis is greatly hindered due to chirality. Therefore, I investigated the ability of curcuphenol analogues to induce expression of the major histocompatibility complex I (MHC-I) in a murine metastatic lung carcinoma cell line *in vitro*. Two derivatives of curcuphenol, P02-113 and P03-97-1, showed improved outcomes *in vitro* and I further evaluated them *in vivo,* as anti-cancer therapeutics. Both compounds reduced tumour burden and increased immune cell infiltration into tumours.

To explore a potential mechanism of P02-113 and P03-97-1, I evaluated them for histone deacetylase (HDAC) inhibition based on structural similarity to established HDAC inhibitors. Upon examination I observed a completely novel effect of enhanced class I/II HDAC activity. Furthermore to identify if this effect was direct and to uncover which HDAC enzymes were being affected, I evaluated individual HDAC enzymes. I discovered that HDAC8 was inhibited by both P02-113 and P03-97-1, however, the activities of HDAC 5 and 10 were enhanced upon treatment.

While the field of cancer immunotherapy has grown, few therapeutics have been identified to target loss of immunogenicity through the up-regulation of the APM. In this thesis two analogues of curcuphenol P02-113 and P03-97-1 have been identified that up-regulate the APM *in vitro* and reduce tumour burden *in vivo*. With these effects P02-113 and P03-97-1 hold great potential as future therapeutics for cancers exhibiting an immunodeficient phenotype through loss of the APM. As well these compounds present

the first class II HDAC enhancers, as they increase the enzymatic activity of HDAC 5 and 10.

Preface

Dr. Wilfred Jefferies conceived screening of novel small molecules to induce the expression of the antigen presentation machinery in collaboration with Dr. Ray Andersen.
TC-1 and A9 cell lines were gifted from the lab of Dr. Michal Smahel.
Initial cellomics and flow cytometry screening of marine extracts was designed by Dr. Lilian Nohara and was performed by Carola Dreier, Jessica O'Keefe-Morrice, Krysta Coyle and Daniel Joo Sung Shim.
$GATA1^{-/-}$ mice were gifted from the lab of Dr. Avery August.
Dr. David Williams completed fractionation and identification of curcuphenol from marine invertebrate extracts.
Dr. Ping Cheng synthesized all curcuphenol analogues.
Lonna Munro assisted with all *in vivo* mouse experiments.
All animal breeding (A14-0267) and experimental (A15-0284) protocols were approved by the UBC Animal Care Committee, which is overseen by the Canadian Council on Animal Care (CCAC).
All experiments were performed under the UBC Biosafety protocol B11-0066.
The Metabolomics Innovation Center (TMIC) at UVIC Genome BC Proteomics Centre designed the pharmacokinetic protocol and analyzed all plasma samples.
Samantha Ellis performed all other work completed in this thesis.

Table of Content

List of Tables

List of Figures

List of Abbreviations

ACT Adopted cell transfer

APC Allophycocyanin

APM Antigen presentation machinery

APP Antigen presentation pathway

BSA Bovine serum albumin

CAR Chimeric antigen receptor

CTL Cytotoxic T lymphocyte

CTLA4 Cytotoxic T lymphocyte associated protein 4

DanCl Dansyl Chloride

DMEM Dulbecco's Modified Eagle's Medium

DMSO Dimethyl sulfoxide

DNA Deoxyribonucleic acid

ER Endoplasmic reticulum

FBS Fetal Bovine Serum

HDAC Histone deacetylase

HDACe Histone deacetylase enhancer

HDACi Histone deacetylase inhibitor

HeLa Human cervical cancer cell line (originating from Henrietta Lacks)

HPV Human papillomavirus

IFN-γ Interferon gamma

i.p. Intraperitoneal

mAb Monoclonal Antibody

MHC-I Major histocompatibility complex class one

MTD Maximum tolerated dose

PBS Phosphate buffered saline

PDL1 Programmed cell death ligand 1

PE Phycoerythrin

PK Pharmacokinetics

RIPA Radioimmunoprecipitation assay

RCF Relative centrifugal force

SEM Standard Error of the Mean

SIRT Sirtuin

TAP Transporter associated with antigen processing

TCR T cell receptor

TIL Tumour infiltrating lymphocyte

TSA Trichostatin A

WB Western Blot

7AAD 7-aminoactinomycin D

Acknowledgements

I would like to thank my committee members Dr. Jan Friedman, Dr. Robert McMaster, and Dr. Keith Humphries for their contributions and endless support throughout this project. I would also like to thank all members of the Jefferies lab, both past and present, for their time, support and patience. Last but not least I want to thank Dr. Wilfred Jefferies for his guidance, support and motivational passion for scientific curiosity.

I dedicate my work to my grandparents, Bud and Patricia, to my parents, Lesli and Bill and to John.

1 Introduction

1.1 Overview

Cancer is a devastating disease that arises from genetic and epigenetic modifications (1-6). A common phenotypic signature seen across several forms of cancer, particularly the deadliest form, metastatic, is loss of immunogenicity and consequently, immune evasion (7-9). This can be achieved through several mechanisms, one of which involves loss of the antigen presentation machinery (APM) (9-11). While the exact mechanisms leading to loss of the APM remain largely unknown and are likely to vary from cancer to cancer, identification of therapeutics that result in restored immune recognition and elimination of cancer cells is desirable. In situations where loss of the APM is attributable to epigenetic modifications such as methylation and acetylation, there is the potential to restore expression by modulating epigenetic enzymes with small molecule drugs. Fortunately the earth has an exceptional abundance and diversity of natural compounds, which could hold the potential as therapeutics through induction of the APM and lead to subsequent elimination of cancer cells.

1.2 Cancer

Cancer accounts for 30% of mortality in Canada, making it the leading cause of death (12). The majority of all cancers arise spontaneously through genetic damage or cell deregulation, which may be initiated by changes in gene sequence, gene expression, epigenetic alterations, or structural variations (1-6). Once a cancer forms its genome mutates at a much higher frequency than normal cells and due to the increased rate of mutational evolution there is a greater chance for primary cancer cells to transition into a more lethal metastatic form (13).

1.2.1 Cancer metastasis

While there are several forms of cancer, they all possess the ability to progress to the deadliest form, metastatic. Metastatic cancer is defined by the ability of cancer cells to spread from a primary site and invade distant tissues (14). This form is of great concern because it is responsible for 90% of all cancer deaths (14-16). Alterations

associated with a cancer's transition into a metastatic form are referred to as the "metastatic gene signature" and include changes in gene expression, epigenetic alterations, and structural variations (16,17). Currently there are several signatures associated with metastatic progression; however, one that is seen across a spectrum of cancers is the loss of immunogenicity (18,19).

1.2.2 Cancer and the immune system

The immune system is critical for maintenance of tissue homeostasis by acting as the primary defense against invading pathogens and damaged or cancerous cells (20,21). There are two different wings of the immune system, innate and adaptive, which differ in the mechanisms through which they protect our bodies. The innate immune system is often referred to as the first responder since it consists of cells and proteins that are always present and can be activated rapidly. Included in the innate system are epithelial barriers, phagocytes (*e.g.* neutrophils, eosiniphils, basophils, mast cells and macrophages), dendritic cells, natural killer (NK) cells and circulating plasma proteins (*e.g.* complement, histamine and cytokines). Alternatively the adaptive immune system, that is antigen specific, becomes activated when pathogens or cancerous cells are able to evade or overcome the innate immune system. The adaptive immune system can be further classified as humoral responses which involves antibodies released by B cells, or cell-mediated responses, which encompasses T cell responses resulting in the elimination of infected or cancerous cells. However, cancer cells can establish mechanisms to evade the cell-mediated wing of the adaptive immune system and avoid destruction (18-21).

This evasive phenotype can be caused by several mechanisms; however, a recurrent cause seen in several cancers, especially metastatic, is the down-regulation of the endogenous APM (22-29). The endogenous APM allows T cells of the adaptive immune system to differentiate among normal cells, virus-infected cells or cancerous cells (30-35). To initiate an adaptive immune response, cytotoxic T lymphocytes (CTLs, CD8+) interact via their T-cell receptor (TCR) with peptides presented on major histocompatibility class I (MHC-I) molecules present on the surface of all nucleated cells (31). Presented peptides are derived from endogenous proteins that are degraded by the proteasome and transported into the endoplasmic reticulum (ER) from the cytosol by the

transporters associated with antigen processing 1 and 2 (TAP-1/2) (34). In the ER peptides are loaded onto the MHC-I molecules before being transported to the cell surface where they are surveyed by the TCR of the CTLs (34). Upon detection of "non-self peptides", the CTLs generate an immune response against the offending cell. However many cancers down-regulate one or all of the proteins involved in the endogenous antigen presentation pathway (APP) through genetic or epigenetic alterations (24-29). The most commonly down-regulated proteins of the endogenous APP are the TAP-1 proteins and the MHC-I molecules, which can become reduced up to 100% in some carcinomas (11, 23, 24).

1.2.3 Regulation of the antigen presentation machinery

While the loss of the endogenous APM is widely seen in cancers, the exact mechanisms leading to its reduction have yet to be fully explained. Previous work in the field has shown that expression of the APM can be re-established in cancer cells through the use of cytokines, a finding suggesting that the loss of MHC-I expression is primarily attributed to deregulation rather than to structural variation (24). Stimulation with interferon- γ (IFN-γ) has shown great success in inducing the expression of the APM *in vitro* (9-11, 28); however, translating this finding into a therapeutic remains difficult, and therapies targeting up-stream regulators are still being explored. Alternatively, treatment with histone deacetylase (HDAC) inhibitors has resulted in re-establishment of the APM and reduced tumour growth *in vivo* indicating that loss of the APM can be a reversible process (9,24,29,36).

1.2.4 Epigenetics and the antigen presentation machinery

Epigenetics is the study of covalent modifications of DNA, RNA, and proteins. In 1983, Feinberg and Vogelstein made the first connection between cancer and epigenetics by comparing DNA methylation in several human cancers and matched normal tissues. During their work they discovered a pattern of reduced methylation in a variety of human cancers (37). Since 1983, the field of cancer epigenetics has vastly grown to include other elements such as RNA and proteins as well as deregulation of other epigenetics marks like acetylation (38-40).

Interestingly, inhibitors of HDACs (HDACi) and to a lesser extent demethylating agents have shown the ability to induce the expression of the APM (10,11, 38). HDACs remove acetyl groups from histone tails, imparting a positive charge and increasing the affinity for the negatively charged DNA, causing tightening of local chromatin structure and reduced transcriptional activity. However, the label of "histone deacetylase" is an oversimplification, as these enzymes are not limited to deacetylation of histones but can also remove acetyl groups from proteins, resulting in a variety of effects that include: subsequent post-translational modifications (such as ubiquitination), increased protein stability, altered subcellular localization, and altered protein-protein interactions (39).

Currently there are 18 known HDACs, which are divided into four classes, I-IV, based on structure and localization. Class I and II HDACs are structurally very similar to each other and operate by zinc-catalyzed hydrolysis, however they differ in their localization (Table 1.2). Class I HDACs are primarily found in the nucleus, are ubiquitously expressed in various tissues and are thought to play a role in cell proliferation. Class II HDACs are found in both the nucleus and cytoplasm and are more selectively distributed in tissues (40). The class III HDACs, known as the sirtuins (1-7), are different from other HDACs as they require nicotinamide adenine dinucleotide for functionality and are not affected by any of the current HDAC inhibitors (40). The final HDAC group, class IV, contains only a single member, HDAC11, which is distinguished from other classes by its small size and prominent localization to the nucleus.

Inhibitors of HDACs fall into four known categories based on chemical structure: hydroxamic acids, cyclic peptides, benzamides, and short chain fatty acids (41). Inhibitors from different categories including Trichostatin A (TSA), Panobinostat, Valporic and Depsipeptide have been shown to up-regulate the APM, however, many of these compounds have not become therapies as there are several concerning off-target side effects (9-11,41,42,43). One major factor in the development of these drugs is their specificity for molecular targets, as many of these compounds are pan HDACi. Therefore it will be essential to identify specific HDAC(s) responsible for the restoration of the APM to create more targeted therapeutics.

1.3 Novel Therapeutics

Natural extracts offer an excellent source of compounds that have potential for HDAC modifying activities. Extracts may be isolated from common daily entities such as spices and herbs or they may come from more distant resources, like plants and animals from the depths of the ocean. While spices are typically thought of as staples in cooking there have been numerous spices identified that have anti-cancerous properties or can reduce tumour growth, and include: saffron, turmeric, green and black tea and flaxseed (44-47). Another common source of natural therapeutics is herbs, which are a rich source of secondary metabolites including: polyphenols, flavonoids and brassinosteriods (48). However, the marine environment dominates all natural resources in its diversity of biologics and chemicals. It has been estimated that 1% of all marine natural products show anti-tumour properties as compared with 0.01% of its terrestrial counterpart (49,50). Of particular interest are marine invertebrates, as roughly 50% of all new FDA approved drugs between 1981 and 2014 were from marine invertebrate metabolites or synthetic analogues (50). Therefore screening of extracts from our natural resources is an important avenue for identification of novel cancer therapeutics.

1.3.1 Curcuphenol

One natural compound of particular interest in regard to cancer therapeutics is a sesquiterpene phenol called curcuphenol. Curcuphenol can be isolated from several sources including marine invertebrates and the commonly used cooking spice turmeric (51). Curcuphenol can be found as one of two enantiomers: S-(+) or R-(-)-curcuphenol (51-59). Of the two enantiomers the S form is known to possess several activities that include: anti-malarial, anti-viral, anti-leishmanial, fungicidal, bactericidal, anti-inflammatory, anti-feedant, anti-fouling, anti-oxidant, and anti-H,K ATPase and anti-Lipoxygenase (51-62).

In relation to cancer studies, S-(+)-curcuphenol has been shown to be cytotoxic to leukemia, lung, breast, leiomyosarcoma, nasopharyngeal and colon cancer cell lines (54,55,60); however, the mechanism(s) underlying this effect remain unknown. It was hypothesized in a previous study using a colon cancer cell line, that S-(+)-curcuphenol worked through a p53-independent mechanism to cause cell cycle arrest and caused

caspase-3 activation, leading to growth inhibition (55). S-(+)-curcuphenol has also been tested for activity against a panel of 24 kinases and was found to inhibit Src kinase, an important kinase known to play a role in enhancing tumour growth and adhesion (63,64). Additionally it has been shown that S-(+)-curcuphenol is an agonist of the free fatty acid receptor 1 (GPR40) that plays a role in proliferation in both breast and pancreatic cancer cell lines (65-68). While these past studies help predict potential pathways through which curcuphenol exhibits its anti-cancer effects, the exact mechanism has yet to be identified. However due to a strong sturcural similarity of curcuphenol to known anti-cancerous compounds, TSA and vorinostat, another potential pathway to be explored in future work is HDAC inhibition.

Interestingly in unpublished data from the Jefferies lab, S-(+)-curcuphenol was identified in a screen of marine invertebrate extracts collected from oceans around the world for the ability to induce TAP-1 and MHC-I expression in murine metastatic lung cell line (69). After identification of extracts with the ability to stimulate expression of the APM, selected extracts were fractionated by separation chromatography and HPLC into aqueous and ethanol fractions in the lab of Dr. Raymond Andersen (Department of Chemistry, UBC). Following fractionation, individual compounds were screened for the ability to induce MHC-I surface expression by flow cytometry. From this screen one fraction showed a significantly stronger induction of MHC-I in comparison to all other tested fractions as well as whole extracts. Using NMR the lab of Dr. Raymond Andersen identified the active compound as S-(+)-curcuphenol. However, synthesis of S-(+)-curcuphenol is limited due to chirality and to overcome this issue several studies have examined synthesis of non-chiral curcuphenol analogues. Analogues have been generated by microbial or chemical modification including hydroxylation, reduction, oxidative cleavage, and esterification, some of which had a positive impact on its biological activities (50,52,57,70,71). Such modifications have allowed researchers to overcome the low yield of S-(+)-curcuphenol and indicates that structural modifications may play an important role in amplifying the anti-cancerous effect of S-(+)-curcuphenol and provides a more productive path towards a future therapeutic.

1.4 Hypothesis and Objectives

1.4.1 Hypothesis

Curcuphenol analogues that induce the antigen presentation machinery *in vitro* will reduce growth of immune evasive tumours *in vivo* through histone deacetylase inhibition.

1.4.2 Determine immune response to TC-1 and A9 *in vivo*

Examine which cells of the immune system are responsible for the identification and elimination of a primary murine lung carcinoma TC-1 and A9 its metastatic derivative with down regulation of the APM *in vivo.*

1.4.3 Identify curcuphenol analogues that induce MHC-I surface expression.

Screen analogues of curcuphenol for induction of MHC-I surface expression in a metastatic murine lung carcinoma with down-regulation of the APM *in vitro*.

1.4.4 Test curcuphenol analogues for the ability to reduce tumour growth and induce cells of the immune system *in vivo.*

Analyze the effect of selected curcuphenol analogues *in vivo* by evaluating tumour growth and immune cell infiltration into the established tumours.

1.4.5 Examine curcuphenol analogues for HDAC inhibition.

Screen curcuphenol analogues for the ability to directly inhibit HDAC activity, due to the structural similarity of curcuphenol and analogues to known anti-cancer compounds that act through HDACi.

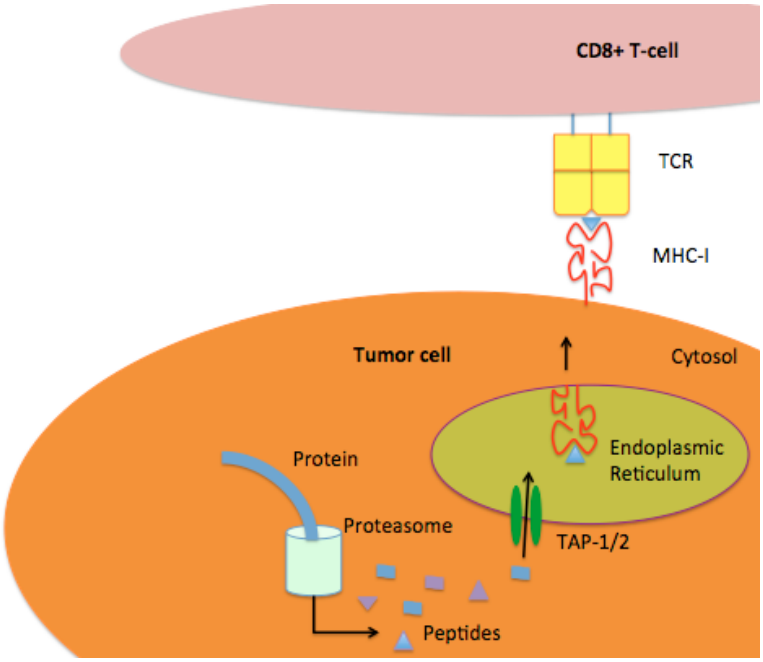

Figure 1.1 Endogenous antigen presentation pathway. The pathway though which endogenous proteins are processed and presented to cytotoxic T lymphocytes ($CD8^{+/+}$) of the immune system via the major histocompatibility complex I molecules.

Table 1. Histone Deacetylase classifications

Class	Enzyme	Accession number	Location
I	HDAC1	CAG46518.1 (h) AAI08372.1 (m)	Nucleus (HDAC8 also in cytoplasm)
	HDAC2	NP_001518.3 (h) NP_032255.2 (m)	
	HDAC3	NP_003874.2 (h) NP_034541.2 (m)	
	HDAC8	AAF73428.1 (h) AAH61257.1 (m)	
II	HDAC4	AAH39904.1 (h) NP_997108.1 (m)	Nucleus/ Cytoplasm
	HDAC5	NP_001015053.1 (h) AAH60609.1 (m)	
	HDAC6	AAH69243.1 (h) AAH41105.1 (m)	
	HDAC7	AAH64840.1 (h) AAH57332.1 (m)	
	HDAC9	AAK66821.1 (h) AAH98187.1 (m)	
	HDAC10	AAL30513.1 (h) AAH13700.1 (m)	
III	SIRT1	AAH12499.1 (h) AAI52315.1 (m)	Nucleus/Cytoplasm
	SIRT2	AAK51133.1 (h) Q8VDQ8.2 (m)	Cytoplasm
	SIRT3	AAD40851.1 (h) Q8VDQ8.2 (m)	Nucleus/ Mitochondria
	SIRT4	AAD40852.1 (h) NP_001161163.1 (m)	Mitochondria
	SIRT5	AAD40853.1 (h) AAH87898.1 (m)	
	SIRT6	CAG33481.1 (h) XP_006513924.1 (m)	Nucleus
	SIRT7	NP_057622.1 (h) AAP83960.1 (m)	
IV	HDAC11	CAG33622.1 (h) NP_659168.1 (m)	Nucleus/Cytoplasm

2 Materials and methods

2.1 TC-1 and A9 Cell Culture

The murine lung carcinoma cell line, TC-1, was derived from primary lung epithelial cells of a C57BL/6 mouse that were immortalized using the amphotropic retrovirus vector LXSN16 carrying the Human Papillomavirus E6/E7 oncogenes and subsequently transformed with pVEJB plasmid expressing the activated human c-Has-ras oncogene (72). The metastatic cell line, A9, is a derivative of TC-1. It was generated *in vivo* after immunization of mice bearing the original TC-1 parental cells in the lab of Michal Smahel and were gifted to the Jefferies lab in 2005 (72). Both cell lines were cultured in Dulbecco's modified Eagle's medium (DMEM, Gibco) containing 10% fetal bovine serum (FBS, Gibco), 100 U/mL penicillin-streptomycin (Gibco) and incubated at 37 °C in a 5% CO_2 humidified atmosphere.

2.2 Western blot

TC-1 and A9 cells were trypsinized (0.05%, Gibco) and washed with Phosphate-buffered saline pH 7.4 (PBS, Gibco). The cells were lysed in RIPA buffer (1xTris buffered saline, Nonidet P40, 0.5% sodium deoxycholate, 0.1 sodium dodecyl sulphate (SDS), 0.004% sodium azide, Santa Cruz Biotechnologies) with HALT protease and phosphatase inhibitor cocktails (Thermo Scientific) on ice for 40 minutes with vortexing every ten minutes. Subsequently, cells were centrifuged at 15,000 x relative centrifugal force (RCF) for 5 minutes and supernatant was collected. Total protein was quantified using a Bradford assay and measured using the Molecular Devices Vmax kinetic micro plate reader. A total of 55µg of protein, in 20µL of 1x NuPAGE SDS sample buffer (Thermo Scientific) was heated to 95 ^{o}C for 5 minutes, before being separated by SDS polyacrylamide electrophoresis (PAGE). Resolved samples were transferred to nitrocellulose membranes (Bio-Rad) before being blocked in 5% (w/v) skim milk with 0.2% Tween 20 (Bio-Rad). The membranes were incubated with rabbit anti-mouse TAP-1 antibody (1:1000 Jackson Immunoresearch Laboratories) and washed three times with PBS containing 2% Tween (Bio-Rad) before incubation with Alexa-Fluor-680 conjugated goat anti-rabbit antibody (1:10,000, Life Technologies). Membranes were

imaged on the Licor Odyssey Imaging System and quantified using Image Studio LITE (LI-COR).

2.3 Flow cytometry

A9 and TC-1 cells were trypsinized (0.05%, Gibco), washed twice with PBS (Gibco), and stained with allophycocyanin (APC) conjugated anti-mouse H-2K^{b} antibody (1:200, Biolegend) suspended in 150µL of FACS buffer (PBS + 2% FBS) for 20 minutes at 4 °C. Cells were washed twice with PBS and re-suspended in 200µL FACs buffer containing 1µL of 7-aminoactinomycin (7AAD) viability stain (Biolegend). Flow cytometry was performed on the LSRII (BDBiosciences) and analysis was done using FlowJo (Flow cytometry Analysis Software).

2.4 Immune response of TC-1 and A9 *in vivo*

The TC-1 and A9 cell lines, were grown in DMEM as previously described in section 2.1, without the addition of antibiotics (penicillin and streptomycin, P/S). Once cells reached 75-80% confluence, they were trypsinized (0.05%, Gibco) and washed with HBSS (Hanks balanced salt solution). The cells were counted using the Bio-RAD TC20 automated cell counter and suspended to a concentration of 10^7 cells/mL in HBSS. To determine the immune-stimulatory properties of cell lines, $5x10^5$ TC-1 or A9 cells were subcutaneously injected into the right flank of 6-8 week syngeneic female C57BL/6 (Jackson Laboratories, Cat#000664) (n=8), CD4$^{-/-}$ (Jackson Laboratories B6.129S2-Cd4^{tm1Mak}*J*, Cat# 002663) (n=8), CD8$^{-/-}$ (Jackson Laboratories, B6.129S2-Cd8 ^{tm1Mak}*J*, Cat #002665) or GATA1$^{-/-}$ (Gifted from the lab of Dr. Avery August; 73) (n=8) mice, giving a total number of 32 mice per cell line. All mouse lines were generated on the C57BL/6 background, and contained null knockouts. Body weights were recorded three times a week following inoculation. Once tumours reached a measurable size (>50mm) they were calibrated three times a week and volume was calculated ($V= L \times W^2$). Mice were euthanized if they reached the humane end point, based on 20% reduction in body weight, a tumour volume larger than 1 cm^3 or ulceration. At a humane end point, final weights and tumour volumes were calculated before mice were euthanized and tumours were removed and weighed.

2.5 Curcuphenol analogues analysis *in vitro*

The original marine extract library was provided by Dr. Raymond J. Andersen (UBC). The marine invertebrate specimens were collected by SCUBA diving at a 40 metre depth from regions of high marine biodiversity in Papua New Guinea, Indonesia, Thailand, Sri Lanka, Dominica, Brazil, British Columbia, South Africa, and Norway. Previously curcuphenol was identified as the active component in one of the marine extracts showing induction of the APM, and since then two new generations of curcuphenol analogues were synthesized in the lab of Dr. Raymond Andersen. To evaluate the ability of these compounds to induce MHC-I surface expression, A9 cells were plated in 6 well plates at 10^5 cells/well and incubated for 24 hours at 37 °C in a 5% CO_2 humidified atmosphere. After 24 hours the medium was removed and replaced with medium containing varying concentration of synthesized compounds (6.7 μg/mL, 20 μg/mL, 60 μg/mL). One positive control, TSA (100 ng/mL), and one negative control (DMEM, 1% dimethyl sulfoxide (DMSO)) were used. Following treatment, cells were incubated for 48 hours at 37 °C with 5% CO_2 and humidified atmosphere. After incubation cells were subjected to flow cytometry following the procedure described in section 2.3.

2.6 Maximum tolerated dose

A total of nine C57B/6 female mice between the ages of 6-8 weeks were used for each compound. The compounds were injected intraperitoneally (i.p.) at concentrations of 1.0 mg/kg (n=3), 3.5 mg/kg (n=3), or 5.2 mg/kg (n=3). The highest dose was based on the maximum solubility of the compounds, which was estimated using the known solubility of curcuphenol. Mice were assessed for clinical signs of toxicity (e.g. weight loss, skin or eye irritation, pain, distress and gait) for 14 days following injection. After 14 days the mice were euthanized and examined by necropsy.

All experimental work involving P02-113 was serviced by The Investigational Drug Program (Department of Experimental Therapeutics, British Columbia Cancer Agency BCCA). I performed all experiments involving P03-97-1, except the necropsy that was serviced by Animal Care Services located at the Center for Comparative Medicine on UBC Point Grey campus, Vancouver BC.

2.7 Pharmacokinetics

To assess the pharmacokinetics (PK) of the curcuphenol analogues, a mass spectrometry assay was developed to measure the compounds in mouse plasma at The Metabolomics Innovation Center (TMIC) at UVic-Genome BC Proteomics Centre located in Victoria, British Columbia. Eight samples, listed in Table 2.1, were sent to TMIC for the PK design. To collect plasma, mice were anesthetised using isoflurane and blood was collected by cardiac puncture. Plasma was isolated from blood in a potassium-EDTA coated Tube with K2E (BD Microtainer) and centrifugation at 10,000 x RCF for 1 minute. Plasma was transferred to a cryovial and stored at -80 ^{o}C before being shipped on dry ice. TMIC used a chemical derivatization – UPLC-MMR/MS method to create a quantitative analysis tool for the compounds using dansyl chloride (Dns.Cl) as the derivatizing reagent. ^{13}C- labeled Dns-Cl.CI was used to produce stable isotope-labeled internal standards (ISs). All tests were performed using an UPLC-4000 QTRAP system with ESI and (+) ion detection using C18 column and acetonitrile-water-formic acid as the mobile phase.

For the PK analysis of P02-113 and P03-97-1, mice were injected i.p. and anesthetised before blood was collected by cardiac puncture at five time points (5 min, 10 min, 30 min, 1 hour and 6 hour). Three female C57BL/6 mice, between the ages 6-8 weeks, were used for each compound for each time point, giving a total 15 mice per compound. Time points were chosen based on the published data for TSA (0.5mg/kg), a drug of similar chemical structure and size to the compounds. All mice were injected at the highest maximum tolerated dose (5.2 mg/kg) and plasma was prepared and stored as previously described above.

2.8 *In vivo* tumour trial

The metastatic cell line, A9, was grown in DMEM as previously described in section 2.1, without the addition of antibiotics (penicillin and streptomycin, P/S). Once cells reached 75-80% confluence, they were trypsinized (0.05%, Gibco) and washed with HBSS (Hanks balanced salt solution). The cells were counted using the Bio-RAD TC20 automated cell counter and suspended to a concentration of 8x10^{6} cells/mL in HBSS. Thirty-two syngeneic female C57BL/6 mice, between the ages 6-8 weeks, were

subcutaneously injected in the right flank with 50μL containing $4x10^5$ A9 metastatic tumour cells. Seven days following tumour inoculation i.p. treatment began daily for 12 days. Four treatment groups were studied, with eight animals per group: the vehicle was used for a negative control (1% DMSO in PBS); and TSA (0.5 mg/kg) a drug known to reduce A9 tumour burden *in vivo* was used as a positive control (9). The treatmennt dose was 5.2mg/kg/d for both P02-113 and P03-97-1. Body weights were taken three times a week. Once tumours developed, they were measured daily with calipers and tumour volume was calculated ($V=LxW^2$). Twelve days after starting treatment, mice were euthanized and tumours were collected and weighed. The tumours were then processed for flow cytometry analysis. Tumours were cut into small pieces and incubated in RPMI (Gibco; with P/S 0.5%, Sodium pyruvate 1%, and L-glutamine 1%) and 3mg/mL collagenase A (Roche) for one hour at 37 °C with shaking. Dissociated tumour cells were passed through a 100 μm filter and spun down at 15,000 x RCF for 3 minutes. The pellet was washed once in FACs buffer (2% FBS in PBS) and spun down. The pellet was next suspended in red blood cell (RBC) lysis buffer and kept at room temperature for 5 minutes before being neutralized by the addition of 5ml of PBS and spun down. If pellets were still found to contain RBCs this step was repeated. Once all RBCs were removed, cells were suspended in FACs buffer to a concentration of 10^7 cells/mL. A total volume of 200 ul of cells from each tumour were added to a 96 well plate (Falcon) and incubated with Fc Blocker (Biolegend, 1:400) for twenty minutes at 4° C. The 96 well plate was spun down at 1,200 rmp for three minutes and supernatant was removed. The cells were then suspended in 150ul of FACs buffer containing anti-CD8a (PE-Cy7, 1:200, eBioscience) and CD4 (APC, 1:200, Biolegend) antibodies and incubated at 4° Celsius for 20 minutes. The cells were washed twice and spun down using FACs buffer before being to flow cytometry tubes in a final volume of 200ul of FACs buffer containing 7AAD (Biolegend 1:200). Flow cytometry was performed on LSRII (BDBiosciences) and analysis was done using FlowJo (Flow cytometry Analysis Software).

2.9 HDAC assays

Compounds P02-113 and P03-97-1 were analyzed for their effect on histone deacetylase activity in the A9 cell line using the HDAC-Glo™ I/II Assay and Screening System (Promega) as instructed by the manufacturer. The linear range of A9 cells was established in a black-walled, clear-bottomed 96 well plate (PerkinElmer). Cells were diluted to 10^5 cells/mL and serial diluted by two fold, to a final concentration of 98 cells/ml. All dilutions were plated in triplicate in a volume of 100ul per well. Cells were cultured at 37 ^{o}C for 24 hours before addition of HDAC class I/II reagent. Luminescence was read after 30-minute incubation with HDAC class I/II reagent. After determination of an optimal cell density of 30,000cells/well, cells were plated in 96 well plate and left for 24 hours at 37 ^{o}C. Medium was used as a blank control, and a positive control provided in the HDAC assay kit was included consisting of HeLa cells. The next day, medium was removed from the wells and new media containing the treatments: vehicle (negative control), TSA (positive control), or a range of dilutions of P02-113 or P03-97-1 (5 to 0.02 μM) were added in triplicate and incubated for 30 minutes. HDAC class I/II reagent was then added and incubated for 30 minutes before luminescence was measured using the Infinite M200 (Tecan) with the i-control software (Tecan).

2.9.1 Individualized HDAC assays

The activity of the curcuphenol analogues was assessed with purified human HDAC enzymes (Table 1) from all classes I, II, and IV, as well as a select member of HDAC class III (SIRT1). HDACs 1-9 and SIRT1 were evaluated using HDAC Fluorogenic Assay Kits (BPS Biosciences). All assays were completed in black-sided clear-bottom 96 well plates (PerkinElmer), and all treatments were plated in triplicate. Treatment started at 5 μM and was two-fold diluted to a concentration 0.02μM. The assays were measured using the Synergy HI hybrid reader (BioTek) and Gen5 software (BioTek); excitation was set to 360nm and detection was measured at 450nm with a gain of 100.

Alternatively, HDAC 10 and 11 (BPS Biosciences) were optimized for HDAC concentration using the HDAC-Glo™ I/II Assay and Screening System (Promega). Following optimization each HDAC was run following the Promega protocol in black-

sided clear-bottomed 96 well plates in triplicates with same treatments listed above (PerkinElmer). Luminescence was read 30 minutes after HDAC-Glo^{TM}I/II reagent was added using the Synergy HI hybrid reader (BioTek) and Gen5 software (Bio-Tek).

For all assays, vehicle (1% DMSO) was used as a negative control and TSA (25nM) was used as a positive control, excluding SIRT1 where nicotinamide (5mM) was used as positive control, and all assays contained blank controls. To calculate percent activity, the average of blank wells was subtracted from all treatment groups. The relative mean of activity of the HDAC being measured was determined, and all wells that received treatment were divided this average, to give a relative percentage of HDAC activity. All individualized enzyme assays were analyzed for significance using an unpaired t-test that compared the different treatment concentrations of the compounds directly to untreated HDACs.

Table 2. Plasma samples sent for development of Pharmacokinetic assay.

SAMPLE	CONCENTRATION (mg/mL)
Plasma from untreated mouse	0
Plasma from untreated mouse with P02-113 added	10
Plasma from untreated mouse with P03-97-1 added	10
Plasma from mouse injected with 100µL of P02-113	10
Plasma from mouse injected with 100µL of P03-97-1	10
100µL of P02-113 in 100% DMSO	13
100µL of P03-97-1 in 100% DMSO	13

3 Results

3.1 Characterization of the TC-1 and A9 cell lines

The murine metastatic lung carcinoma cell line, A9, known to have reduced expression of the APM, was chosen for the analysis of small molecules to recover an immunological phenotype (Figure 3.1)(9-11, 68). The metastatic A9 cell line was derived from a murine primary lung carcinoma, TC-1 that retains expression of the APM, by passaging *in vivo*

3.1.1 Immune response *in vivo*

To determine if there was a difference in immune response to primary and metastatic cell lines *in vivo,* $5x10^5$ TC-1 cells were subcutaneously injected into the right flank of a variety of 6-8 week old, syngeneic mouse models. To assess the induction of both the endogenous and exogenous pathways of the APM, mice lacking either CTLs ($CD8^{-/-}$, n=8) or T helper cells ($CD4^{-/-}$, n=8) were inoculated. Control mice with fully capable immune systems (wild type C57BL/6 mice, n=8) were also included, as well as mice lacking eosinophils ($GATA1^{-/-}$, n=8) that are a class of immune cells known to play a role in tumour response. All mice inoculated with the TC-1 cell line were weighed three times a week throughout the study, and it was found that all mice gained weight at a healthy rate with no significance difference between any of the four groups (Figure 3.2A). Of the four-mouse strains, mice lacking CTLs developed the largest tumours in comparison to the wild type controls (Figure 3.2B&C)(p-value<0.0001), demonstrating that the CTLs play a crucial role in recognizing the TC-1 cells and reducing overall tumour burden. This was as hypothesized as CTLs interact with cancer cells via the MHC-I molecules, validating the important role of the endogenous antigen pathway in adaptive immune system's identification and elimination of cancer cells.

The mouse model lacking T helper cells, representing the exogenous APM that acts through MHC-II molecules, also showed a more significant tumour weight than the wild type controls (Figure 3.2 B&C)(p-value=0.018). A possible explanation for this difference is that the T helper cells are known to help maintain CTL activity after initial activation, and upon removal of the T helper cells the CTLs may have lost a significant

amount of activity. The final mouse model examined, lacking eosinophils, had no significant difference from the wild type mice.

The same mouse experiment was performed using the A9 cell line. Mice of all four genotypes developed tumours at a similar rate when inoculated with A9. However, due to the aggressive nature of the A9 cell line, several mice developed ulcerations and had to be euthanized; and to keep the time of tumour growth consistent all mice were sacrificed on day 14. Of the mouse models examined, only mice lacking T helper cells showed a difference in tumour burden compared to wild type controls (Figure 3.3), however, the difference was still not found to be significant. As for the other knockout models examined, there was no significant difference in tumour burden in comparison to the wild type mice (Figure 3.3) demonstrating that eosinophils are not involved in response to these cell lines and that MHC-1 and TAP-1 expression is required for a CTL response *in vivo.*

3.2 Screening small molecules for induction of MHC-I

Two generations of curcuphenol analogues were evaluated for their ability to induce MHC-I surface expression *in vitro*. Analogues showing the greatest induction of MHC-I and lowest cytotoxicity were further examined for effects on tumour growth *in vivo*.

3.2.1 Identifying curcuphenol analogues that induce MHC-I *in vitro*

While curcuphenol was previously isolated from a sea sponge extract in the pure S enantiomer, laboratory synthesis of curcuphenol results in a racemic mixture necessitating cumbersome separation methods. Instead, we opted for the synthesis of analogues lacking the chiral center and two generations of curcuphenol analogues were synthesized in the laboratory of Dr. Raymond Andersen. The first generation was modified by structural changes to the carbon tail, P02-113 and P02-116, whereas the second generation contained modifications on both the carbon tail as well as the carbon ring, P03-93, P03-97-1, P03-97-2 and P03-99. Compounds were screened by flow cytometry for the ability to induce MHC-I expression at the cell surface of A9 cells while maintaining a low level of cytotoxicity (Figure 3.4A). Two analogues, P02-113 and P03-

97-1, were particularly interesting due to their reproducibility for strong induction of MHC-I while maintaining low cytotoxicity (Figure 3.4B).

3.2.2 Maximum tolerated dose

To determine the maximum tolerated dose of the curcuphenol analogues, P02-113 and P03-97-1 in mice, they were evaluated for toxicity at increasing concentrations. The initial concentration was 1.0 mg/kg for both compounds, followed by 3.5 mg/kg and a final concentration of 5.2 mg/kg. Compounds were dissolved in PBS with 1%DMSO, which was a limiting factor as they require a higher percentage of DMSO to be dissoved at concentraions greater then 5.2mg/kg; and 1% DMSO is the highest concentration approved for i.p. injection. Three mice were evaluated at each concentration for both compounds, giving nine mice per compound. Mice were monitored for 14 days and no clinical signs of toxicity were seen. At 14 days, mice were subjected to necropsy. For all concentrations both compounds showed no signs of toxicity or internal abnormalities. Therefore 5.2 mg/kg was chosen for dosing in future experiments.

3.2.3 Pharmacokinetics of P02-113 and P03-97-1

To determine the dosage regimen for treatment of mice, the pharmacokinetics of P02-113 and P03-97-1 were monitored after i.p. injection at varying time points. Time points were chosen based on the literature from a structurally similarity compound, TSA, which becomes metabolized by reduction, *N*-demethylation, and oxidation between 5 and 60 minutes with a half-life just under ten minutes and no detection after 24 hours (74). While the analogues are similar to each other in structure, they were significantly different in their metabolism (Figure 3.5). P03-97-1 was found in mouse plasma at 30 ng/mL at 5 minutes, 18 ng/mL at 10 minutes, 4.0 ng/mL at 30 minutes, 1.0 ng/mL at an hour and became undetectable after 6 hours. In contrast P02-113 was found in mouse plasma at 0.4 ng/mL at 5 minutes, 0.2 ng/mL at 10 minutes, 0.055 ng/mL at 30 minutes, 0.05 ng/mL at 1 hour and became undetectable after 6 hours. Due to time limitations in the ability to inject mice and collect blood no time points earlier then 5 minutes were possible. Another limitation was that each time point required one mouse to get sufficient plasma for PK sampling, therefore one mouse could not be used for multiple time points.

Both compounds were consistent in that they reached undetectable levels in mouse plasma at the 6-hour time point. Due to undetectable levels of both compounds in mouse plasma after 6 hours, which is similar to TSA, a compound that is effective upon daily dosing, I chose to treat the mice daily.

3.2.4 Evaluation of small molecules P02-113 and P03-97-1 *in vivo*

To evaluate the ability of the small molecules to stimulate the immune system *in vivo,* A9 cells were subcutaneously injected into the right flank of 32 6-8 week old C57BL/6 mice at a concentration of $4x10^5$cells/mouse. Seven days after inoculation mice were randomized into one of four treatment groups (n=8): vehicle (1% DMSO), TSA (0.5mg/kg), P02-113 (5.2.mg/kg), or P03-97-1 (5.2mg/kg), and treated daily by i.p. for 12 days. The body weights and tumour volumes were measured three times a week throughout the entire study. In all four treatment groups, body weights remained stable throughout the study (Figure 3.6A). The tumour volumes (Figure 3.6B) were reduced in the TSA, P02-113 and P03-97-1 treatment groups compared to the vehicle control. Tumour weights (Figure 3.6C) were measured at the end point and found to agree with final tumour volume data collected at the end of the study. While none of the treatments exhibited statistically significant results when calculated by two-tailed students t-test, P03-97-1 exhibited the strongest anti-tumour effect.

Tumours were also subject to analysis for T cell infiltration at the study end point. Tumours were analyzed by flow cytometry for CD4+ (APC) and CD8+ (PE-Cy7) T cells (Figure 3.7). Interestingly, the infiltration of CD8+ T cells followed a similar pattern to what was seen in tumour burden. TSA and P03-97-1 were associated with the greatest CD8+ infiltration followed by P02-113 and vehicle alone. As for the CD4+ there was no significant infiltration or difference in any of the groups. These results suggest that P03-97-1 was a stronger immunological stimulator *in vivo* and also exhibited greater reduction in tumour burden.

3.3 Class I/II HDAC activity

Due to structural similarity of the curcuphenol analogues, P02-113 and P03-97-1 to a previously described HDACi, TSA, it was hypothesized that these molecules could be acting through a similar mechanism. To test this theory P02-113 and P03-97-1 were analyzed in the A9 cell line using a general HDAC-Glo^{TM} I/II Assay and Screening System (Promega). First, the linear range of HDAC enzyme activities in the A9 cell line was determined for optimal fluorescence reading in the assay, and a density of 30,000 cells/mL was selected (Figure 3.8A). Following optimization, the small molecules were tested in a range of concentrations (1nM-1uM) on the metastatic murine lung carcinoma cell line, A9, following the assay protocol and luminescence was determined.

Interestingly the compounds P02-113 and P03-97-1 exhibited the opposite effect to what was hypothesized and showed an increase in class I/II HDAC activity (Figure 3.8B). Even at the lowest concentrations, 1 nM-100 nM, there was an induction of HDAC activity. Both compounds showed a peak in HDAC activity around 180 nM, while P02-113 showed a reduced effect at higher concentrations. Alternatively the positive control, TSA, was found to inhibit class I/II HDACs to a level of almost zero activity at all concentrations tested.

3.4 Class I HDAC activity

In the class I HDAC family there are four HDACs, 1,2,3 and 8. Of the class I HDACs tested, 1-3 showed no significant change in HDAC activity at the concentrations tested for both P02-113 and P03-97-1 (Figure 3.9). For compound P02-113, HDAC8 showed more variable results (Figure 3.10), with no change in HDAC8 activity at higher concentrations but at concentrations of 0.3uM and below inhibition was seen, similar to the HDACi exhibited by TSA. P03-97-1 also followed a similar pattern with no change in activity at higher concentrations but at the lowest concentration 0.02uM an inhibitory phenotype was seen. This indicates that the analogues P02-113 and P03-97-1 act as inhibitors to HDAC8 but not for other class I enzymes. Another interesting factor that correlates with the inhibitory effects of P02-113 and P03-97-1 is that HDACs 1-3 are limited to the nucleus whereas HDAC8 is the only class I also found in the cytosol.

3.5 Class II HDAC activity

The class II HDAC family encompasses HDACs 4 through 10 excluding HDAC8. All class II HDACs were evaluated with compounds P02-113 and P03-97-1 at concentrations ranging from 0.02 to 5 μM. Of the class II HDACs, those that showed no significant change in activity upon treatment were HDACs 4, 6, 7 and 9 (Figure 3.11). Of these HDACs, it is also noteworthy that although TSA was used as a positive control it is known that TSA has a limited effect on HDACs 6, 7 and 9, indicating these HDACs may have more unique structures making them a harder target when looking for compounds to alter HDAC activity. In contrast both HDAC 5 and 10 were enhanced upon treatment with either of the curcuphenol analogues (Figure 3.12). For HDAC5, it was seen that enhancement was limited to concentrations between the range 2.5- 0.01 μM for both P02-113 and P03-97-1. The most significant change in activity for P02-113 ($p < 0.001$) was at concentrations 0.04 μM and 0.07 μM, whereas for P03-97-1 the most significant enhancement was at 0.02 μM, 0.04 μM and 0.15 μM ($p = 0.0001$-0.0007). HDAC10 was enhanced at all concentration between 5- 0.04 μM for both compounds, indicating that a wider concentration range is needed to determine the limits of dosage on HDAC10 enhancement. For HDAC10, P02-113 demonstrated lower significance for all tested concentrations tested ($p = 0.0105$-0.0488) then P03-97-1 which peaked at concentrations 0.15 μM ($p=0.0048$) and 0.07 μM ($p=0.0062$).

3.6 Class III HDAC activity

There has yet to be an HDACi that has an effect on the class III enzymes; therefore only one enzyme was selected for analysis of activity upon treatment with the two analogues. SIRT1 was chosen because it is the only class III enzyme that is known to play a role in carcinogenesis. SIRT1 was treated with compounds P02-113 and P03-97-1 between the range of 5μM and 0.02 μM and did not produce a change in activity upon treatment (Figure 3.13). Due to this result and strong similarity in structure to other class III enzymes, no further class III enzymes were tested.

3.7 Class IV HDAC activity

The activity of HDAC11, the only class IV enzyme, was unaffected upon treatment with either analogues P02-113 or P03-97-1 between the range of 5μM and 0.02 μM (Figure 3.14). This indicates that the compounds neither enhance nor reduce the activity of HDAC11 at the examined concentrations.

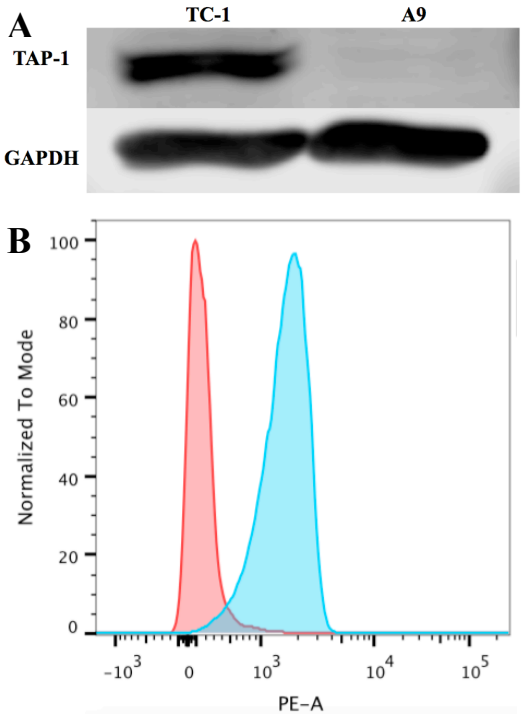

Figure 3.1 Characterization of antigen presentation machinery proteins, TAP-1 and MHC-I, in TC-1 (primary) and antecedent A9 (metastatic) cell lines *in vitro*.
(A) Levels of TAP-1 protein measured by Western blot in TC-1 and A9 cell lines. **(B)** Surface expression levels of MHC-I (PE-A) on TC-1 (blue) and A9 (red) cell lines measured by flow cytometry.

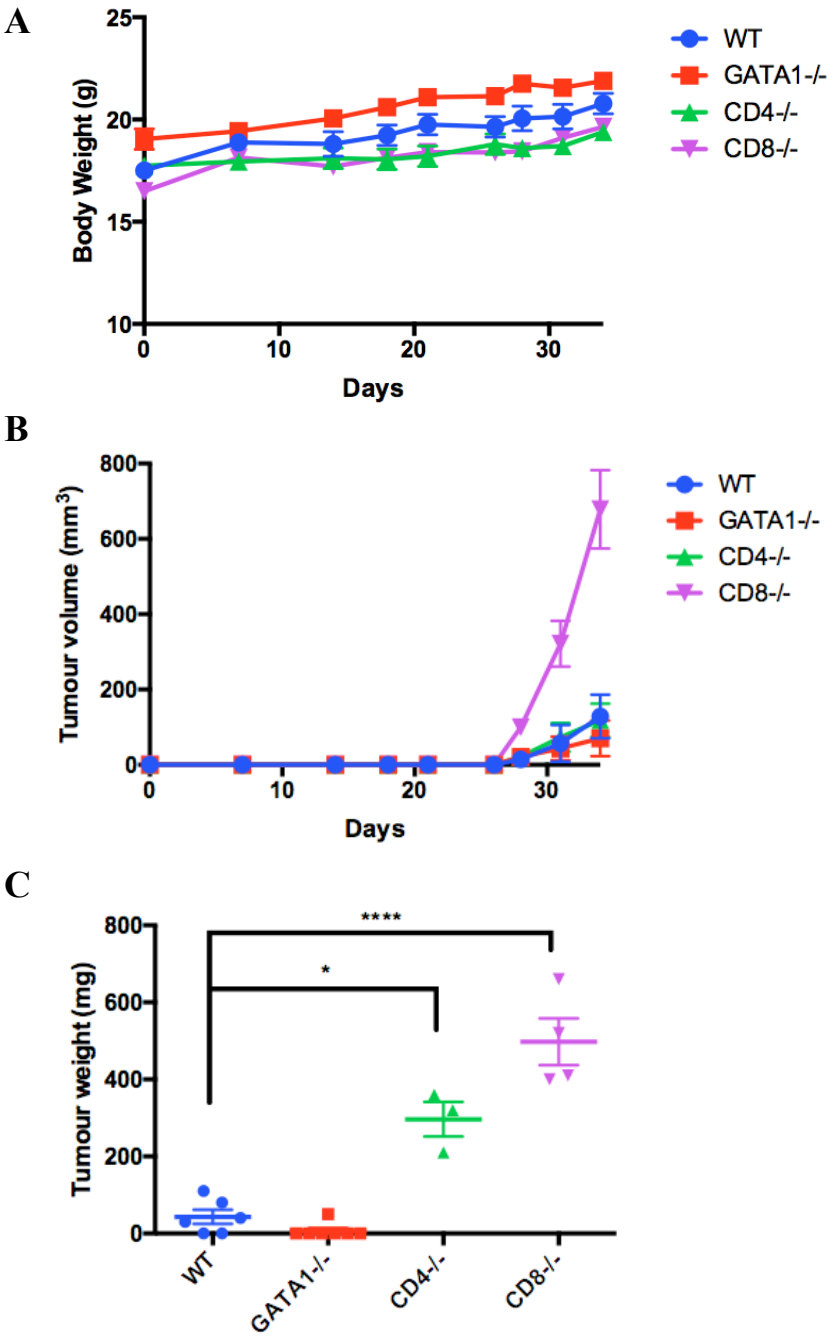

Figure 3.2 Characterization of immune response to the TC-1 cell line *in vivo*.
To examine the immunological characteristics of the TC-1 cell line *in vivo* $5x10^5$ cells were subcutaneously injected into the right flank of 32 mice: C57BL/6 (n=8), $GATA1^{-/-}$ (n=8), $CD4^{-/-}$ (n=8), and $CD8^{-/-}$ (n=8). **(A)** Mean body weight for each group was recorded three times a week until humane end point and plotted with standard error. **(B)** Tumour volume was measured three times a week ($V=L \times W^2$) and mean and standard error was calculated. **(C)** After 34 days all mice were euthanized and mean tumour weights and standard error (SEM) was determined. Outliers were removed if two SEM outside the average calculated for each group. The tumour volumes of $CD8^{-/-}$ mice were found to be significantly larger then wild type mice (p-value <0.0001), when analyzed by unpaired t-test. The $CD4^{-/-}$ mice also showed a significant increase (0.018) in tumour volume when compared to wild type using an unpaired t-test analysis.

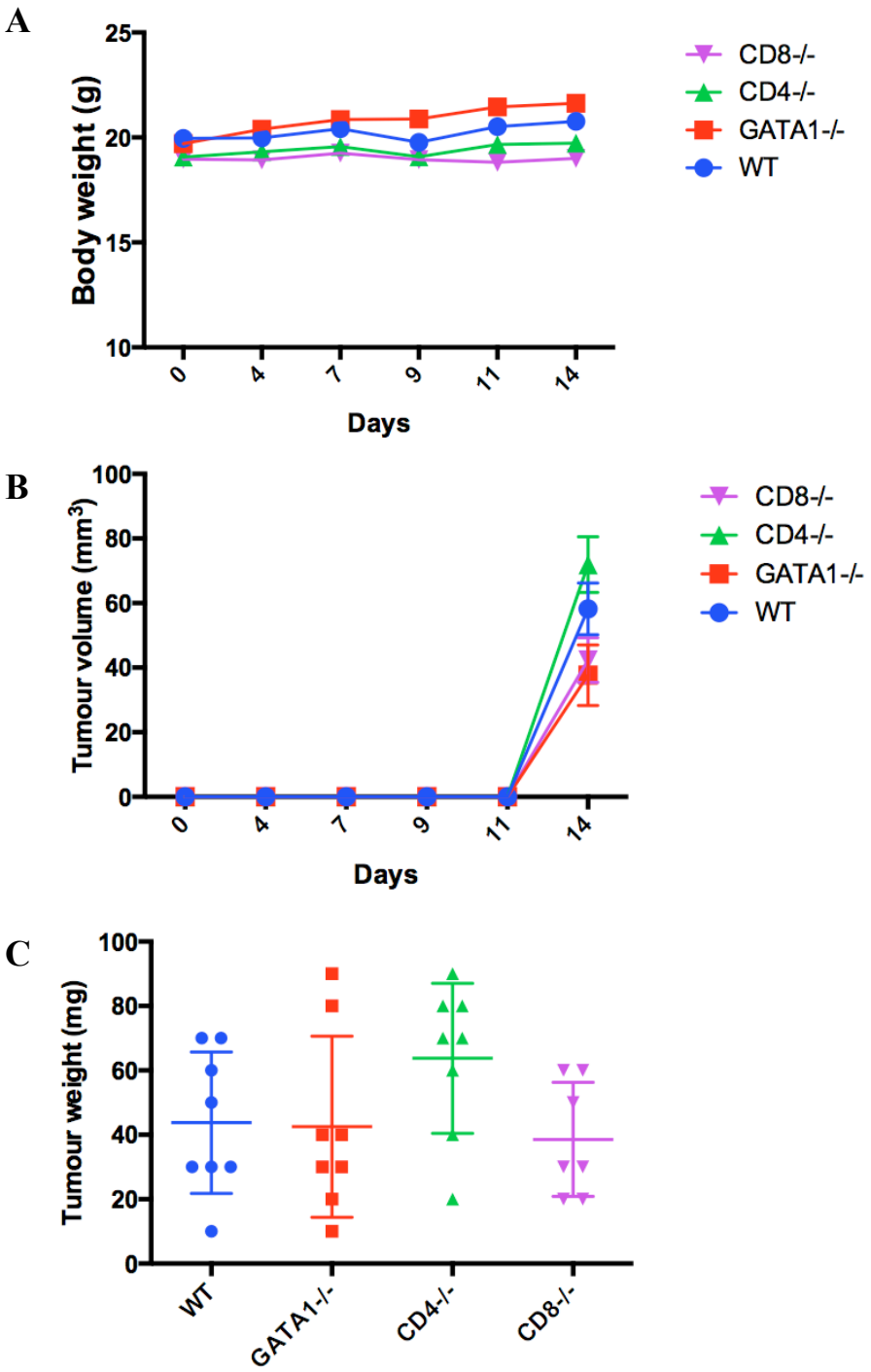

Figure 3.3 Immune response to A9 cell line *in vivo*.
To examine the immunological characteristics of the A9 cell line *in vivo* $5x10^5$ cells were subcutaneously injected into the right flank of 32 female mice: C57BL/6 (n=8), $GATA1^{-/-}$ (n=8), $CD4^{-/-}$ (n=8), and $CD8^{-/-}$ (n=8). **(A)** Mean body weight were recorded three times a week until humane end point for all groups and SEM was calculated. **(B)** Tumour volume was measured three times a week ($V=L \times W^2$) and mean and standard error were determined. **(C)** After 14 days all mice were euthanized and mean tumour weights were determined and SEM was calculated; outliers were removed if two SEM outside the average calculated for each group. No significant difference in tumour volume was observed for any of the models in comparison to wild type using an unpaired t-test.

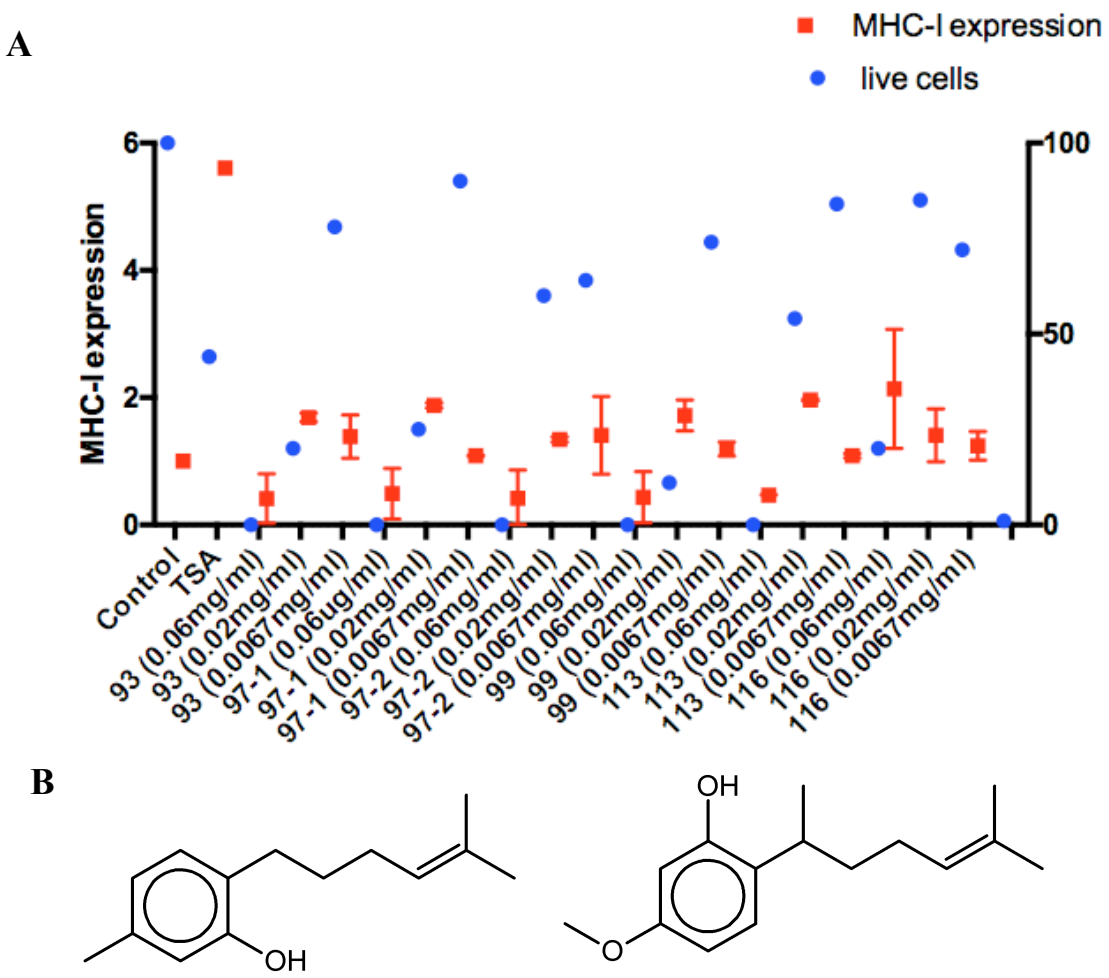

Figure 3.4 Screening of two generations of curcuphenol analogues for induction of MHC-I on the cell surface of A9 cell line *in vitro.* (A) Cells were plated (Day 0) at a density of 10^5cells/well in a 6 well plate. After 24 hours they were treated with one of curcuphenol analogues at a range of concentrations (0.0067 mg/mL, 0.02 mg/mL, or 0/06mg/mL). After 48 hours the cells were analyzed by flow cytometry expression of MHC-I at the cell surface with standard error. **(B)** Structure of P02-113 and P03-97-1.

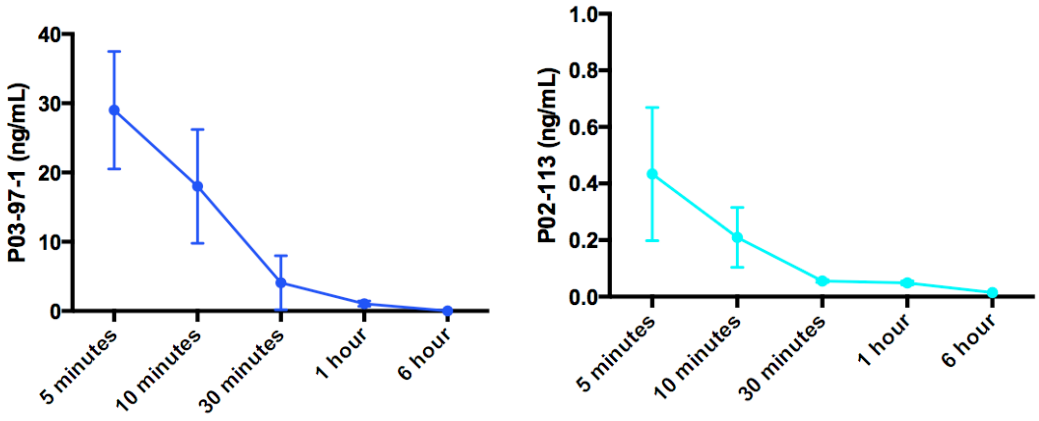

Figure 3.5 Pharmacokinetic analyses of P02-113 and P03-97-1. Mean concentration of P02-113 and P03-97-1 in mouse plasma from three mice at each time point are plotted with SEM. Female C57BL/6 mice, between the ages of 6-8 weeks, were i.p. injected with 5.2 mg/kg of P02-113 or P03-97-1 and blood was collected by cardiac puncture from mice at various time points (n=3) following injection. Plasma was isolated from blood and shipped on dry ice, to TMIC for PK analysis.

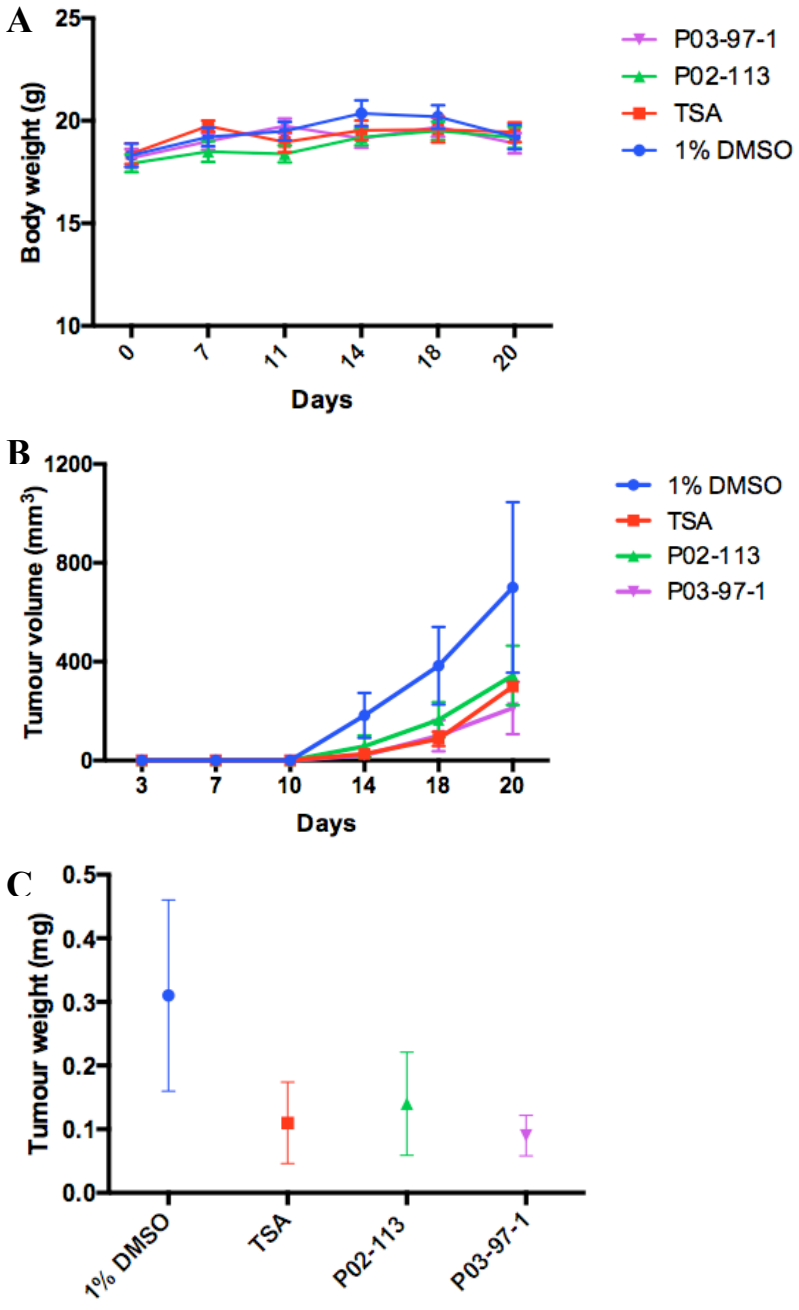

Figure 3.6 *In vivo* analyses of anti-cancer effects of P02-113 and P03-97-1. Thirty-two C57BL/6 mice were injected subcutaneously in the right flank by i.p. with 4 x 10^5 A9 cells. After seven days mice were randomized into four treatment groups (8 mice per group): vehicle (1% DMSO), TSA (0.5mg/kg, positive control), P02-113 (5.2mg/kg), or P03-97-1 (5.2mg/kg), and were treated daily for twelve days. **(A)** Mean body weights and **(B)** mean tumour volumes were calculated ($V=L \times W^2$) three times a week and SEM was determined. **(C)** Following 12 days of treatment mice were euthanized and tumours were removed and weighed, mean tumour weights are plotted with SEM. There was no significant difference seen between mean tumour volumes between any of the treatment groups and the vehicle control using unpaired t-test.

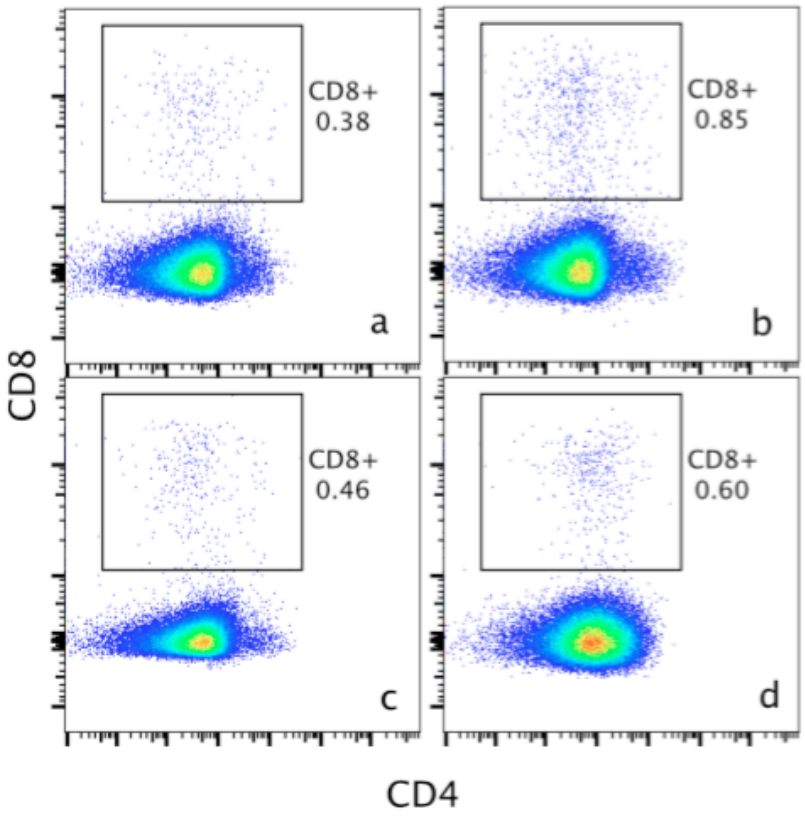

Figure 3.7 Analysis of T cell infiltration of tumours *in vivo.*
C57BL/6 mice were injected with 4 x 10^5 A9 cells, subcutaneously in the right flank. Seven days after injection mice were divided into four treatment groups: vehicle **(a)**, TSA (0.5mg/kg) **(b)**, P02-113 (5.2mg/kg)**(c)**, or P03-97-1 (5.2mg/kg)**(d)**. Following 12 days of treatment tumours were removed and analyzed by flow cytometry for anti-CD4+ (APC) and anti-CD8+ (PE-Cy7) infiltration.

A

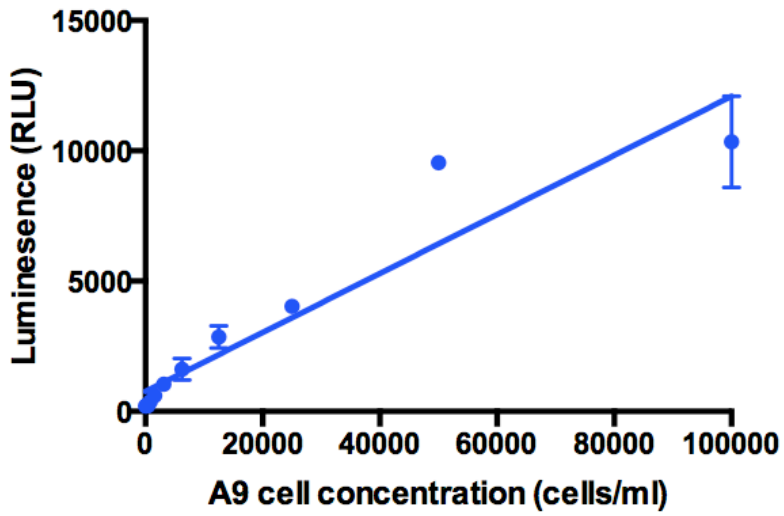

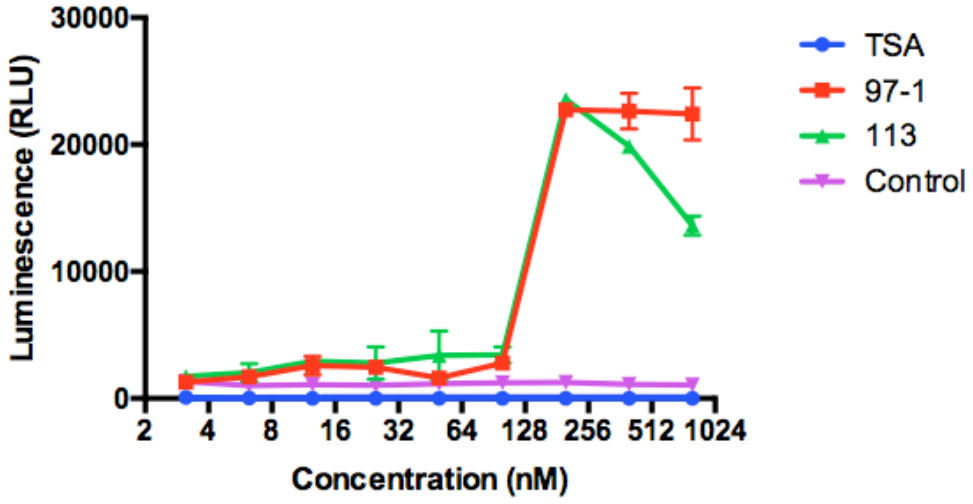

Figure 3.8 Class I/II histone deacetylase assay measuring HDAC activity in A9 cells after treatment with P02-113 or P03-97-1. The HDAC-Glo™ I/II Assay and Screening System (Promega) was used to measure the effect of P02-113 and P03-97-1 on the activities of class I/II HDACs on the A9 cells *in vitro*. The linear range of the A9 cells was first determined following the assay protocol **(A)**. After optimization of A9 cell density the cells were plated at a concentration of 30,000 cells/ml and left overnight at 37° Celsius. The cells were then treated with vehicle, TSA (50nM), or a range of concentrations of P02-113 or P03-97-1. After completing the assay following the screening protocol the fluorescence was measured using the Infinite M200 (Tecan) with i-control software (Tecan) with standard error. From the screen it was seen that the mean activity class I/II HDACs was increased at all treatment concentrations with P02-113 and P03-97-1, a completely novel function of classI/II HDAC enhancement.

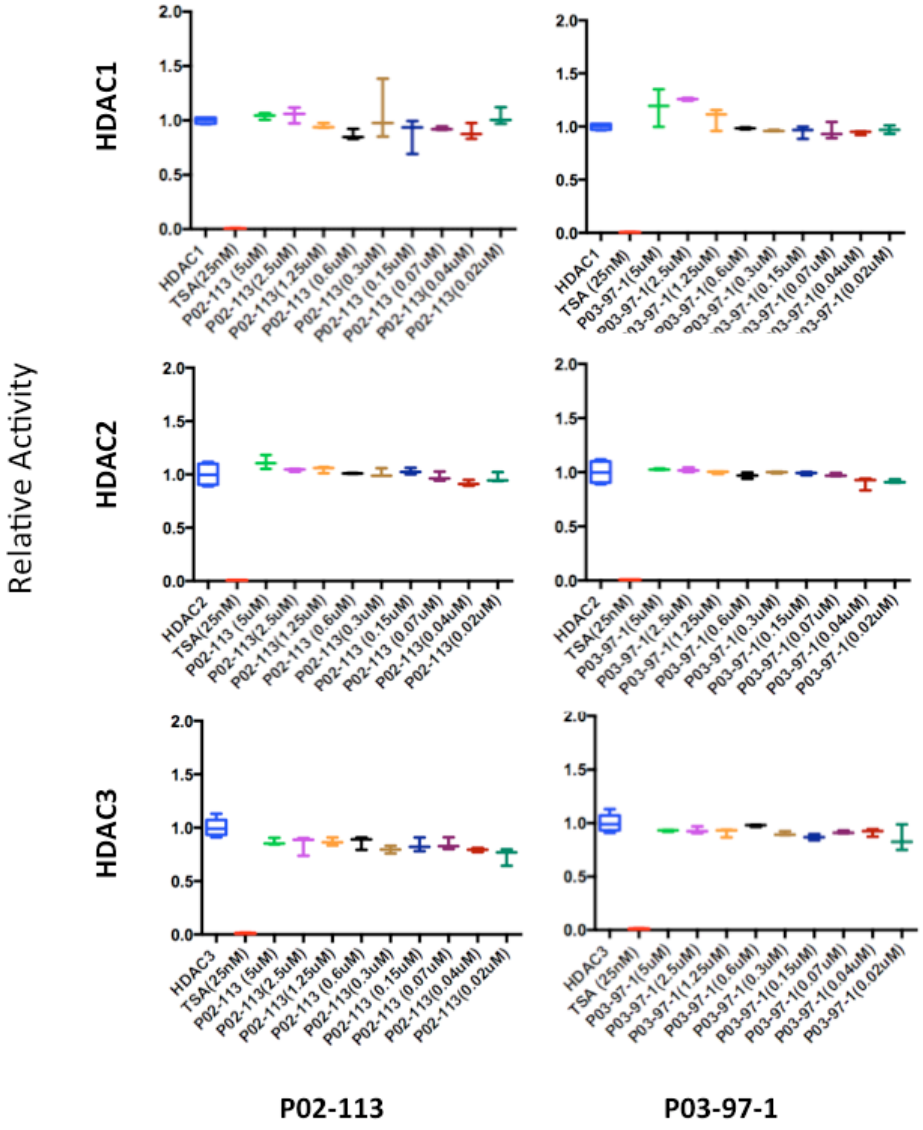

Figure 3.9 Class I HDAC enzymes unaffected by P02-113 or P03-97-1. The Class I HDACs were evaluated for mean activity with standard error after treatment with P02-113 or P03-97-1 using the respective HDAC fluorogenic kits (BPS Biosciences). HDACs 1-3 showed no significant change in activity upon treatment with either P02-113 or P03-97-1 at concentrations ranging from 5μm to 0.02μm using an unpaired t-test.

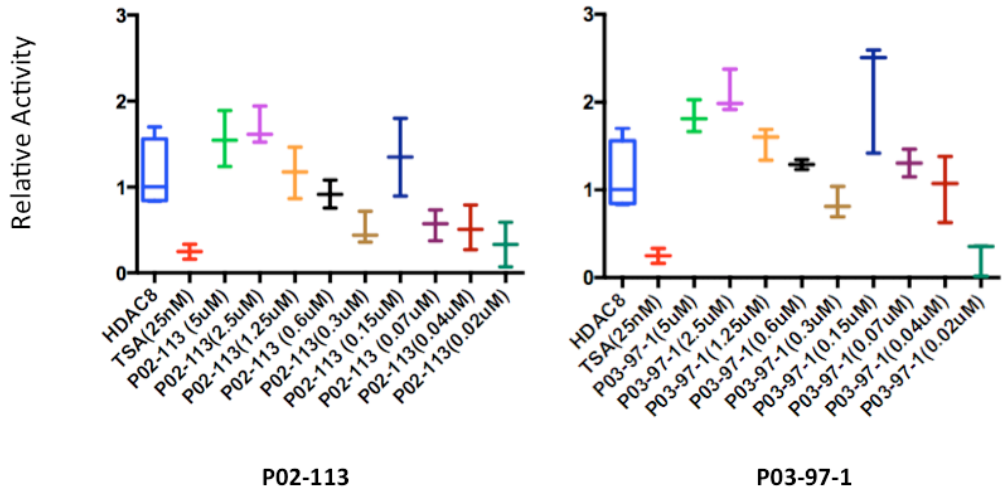

Figure 3.10 HDAC8, a class I HDAC, showed a decrease in activity when exposed to P02-113 or P03-97-1. HDAC8 enzyme activity was measured using a HDAC8 fluorogenic kit (BPS Biosciences). Upon treatment with P02-113 and P03-97-1, HDAC8 showed inhibition at the lower treatment concentrations.While there was a decrease in activity for both compounds, neither was significant when calculated using an unpaired t-test based on mean and standard error.

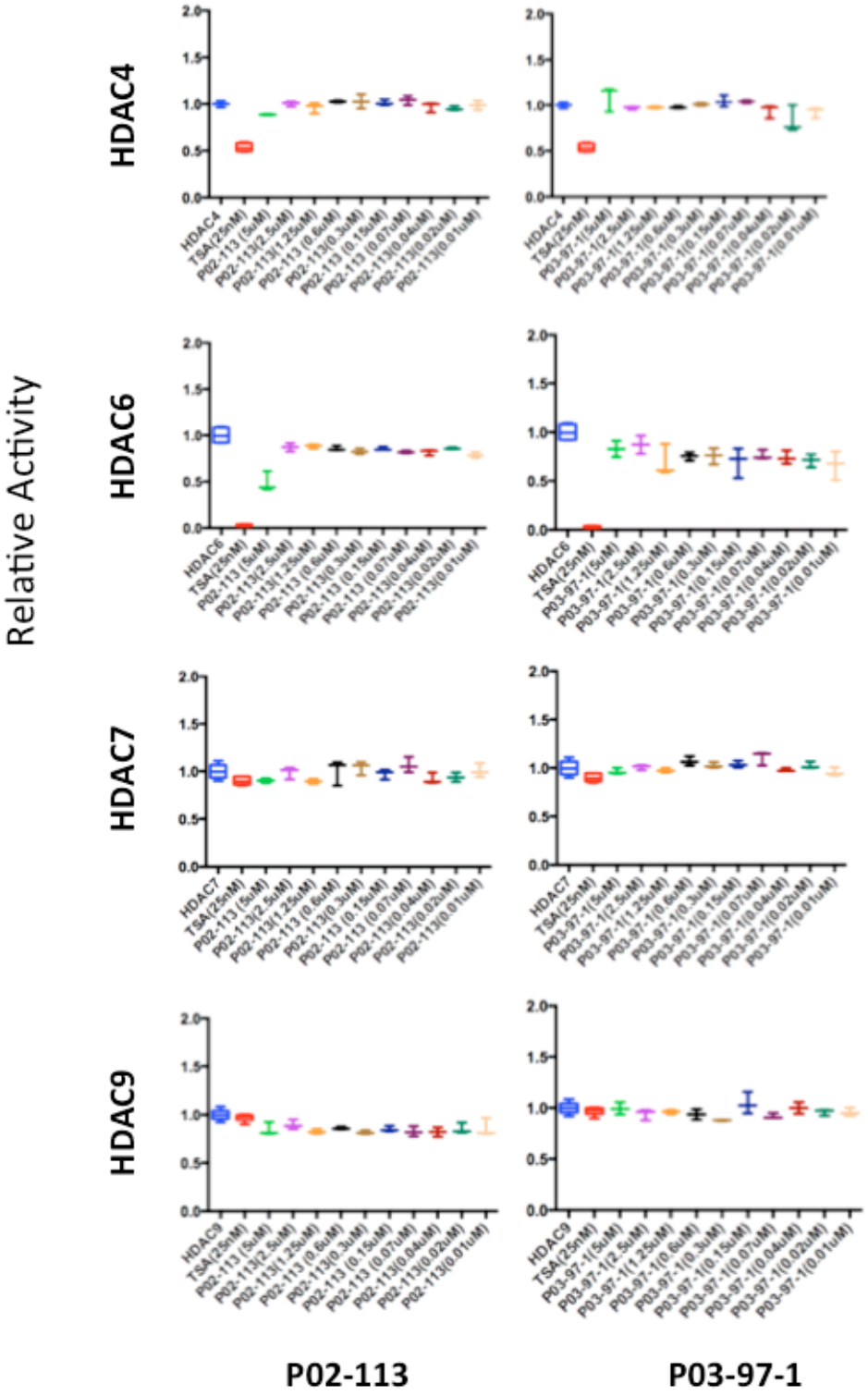

Figure 3.11 HDAC class II Fluorogenic assay of HDACs unaffected by P02-113 or P03-97-1. HDACs 4,6,7,and 9 did not show a significant difference in mean activity with standard error upon treatment with analogues between the concentrations 5 µm to 0.02, determined by an upaired t-test. HDACs 4,6,7 and 9 were measured using the respective fluorogenic kits (BPS Biosciences).

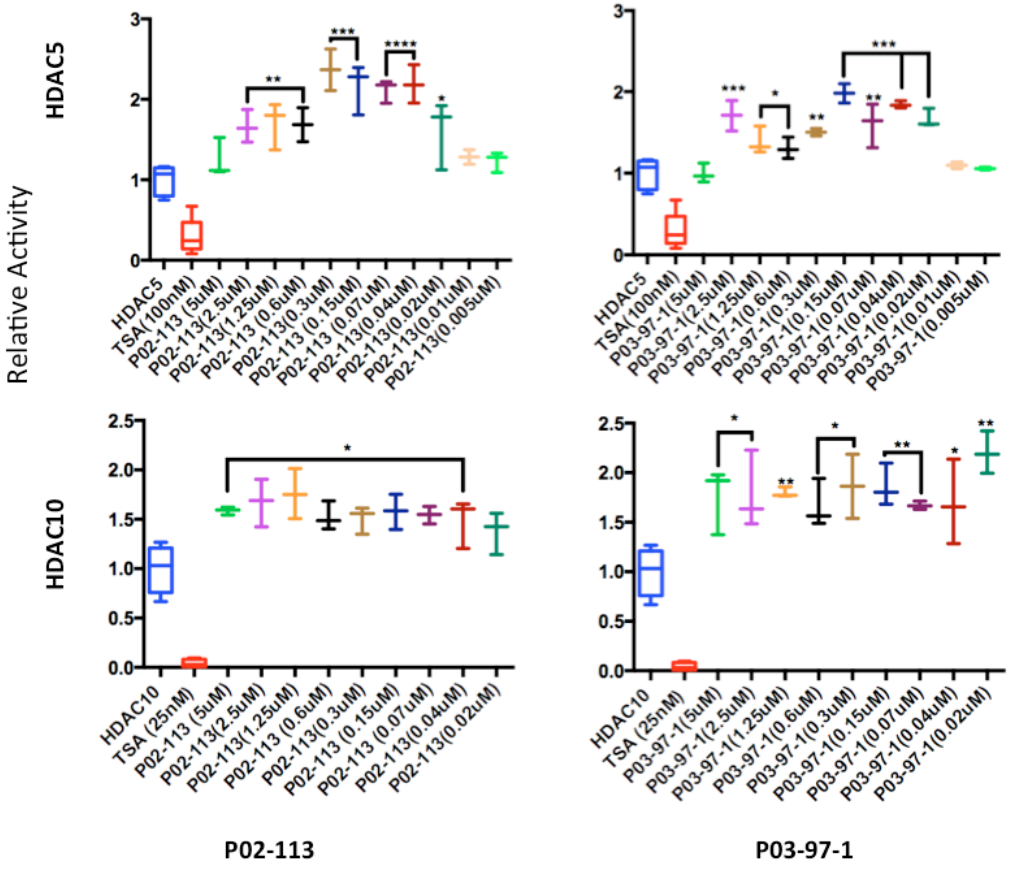

Figure 3.12 Class II HDAC assays of HDACs with enhanced activity upon treatment with either P02-113 or P03-97-1. HDAC 5 and 10 were the only class II HDACs showing an increase in mean activity levels with standard error upon treatment with curcuphenol analogues. HDAC10 was enhanced at all concentrations tested, while HDAC5 showed limitated enhancement between the concentrations of 0.02-2.5 μM, for both compounds. Although both compounds were shown to be significant by unpaired t-test, they were found to have a more significant effect in HDAC5. HDAC5 activity was measured using a HDAC5 fluorogenic kit (BPS Biosciences) and HDAC10 was measured using the HDAC-Glo™ I/II Assay and Screening System (Promega).

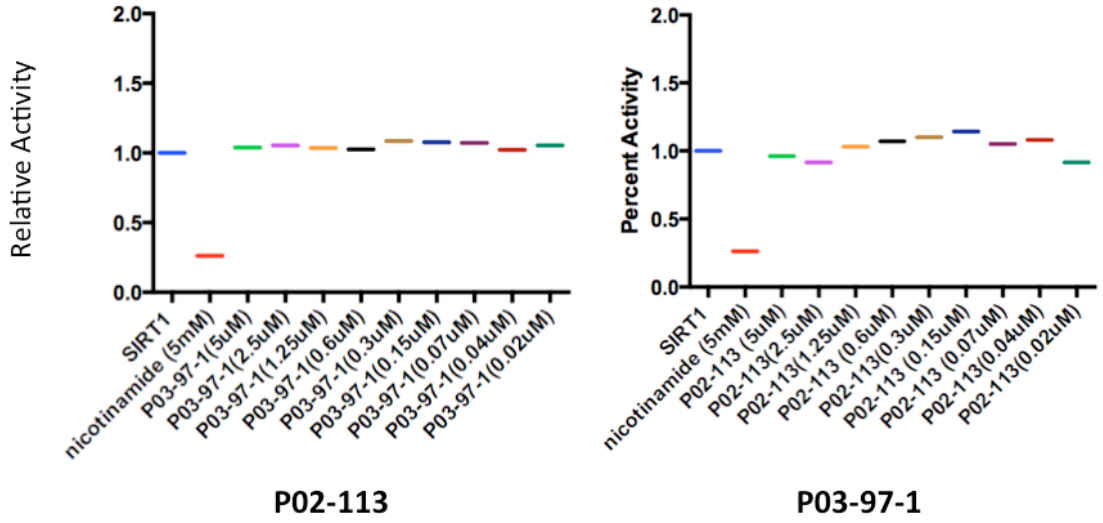

Figure 3.13 Analysis of SIRT1 activity, from the class III HDAC family, after treatment with P02-113 or P03-97-1. SIRT1 activity was measured using the SIRT1 fluorogenic kit (BPS Biosciences). SIRT1 showed no change in activity upon treatment with P02-113 or P03-7-1 between the concentrations of 5µm to 0.02µm determined by an unpaired t-test using mean and standard error.

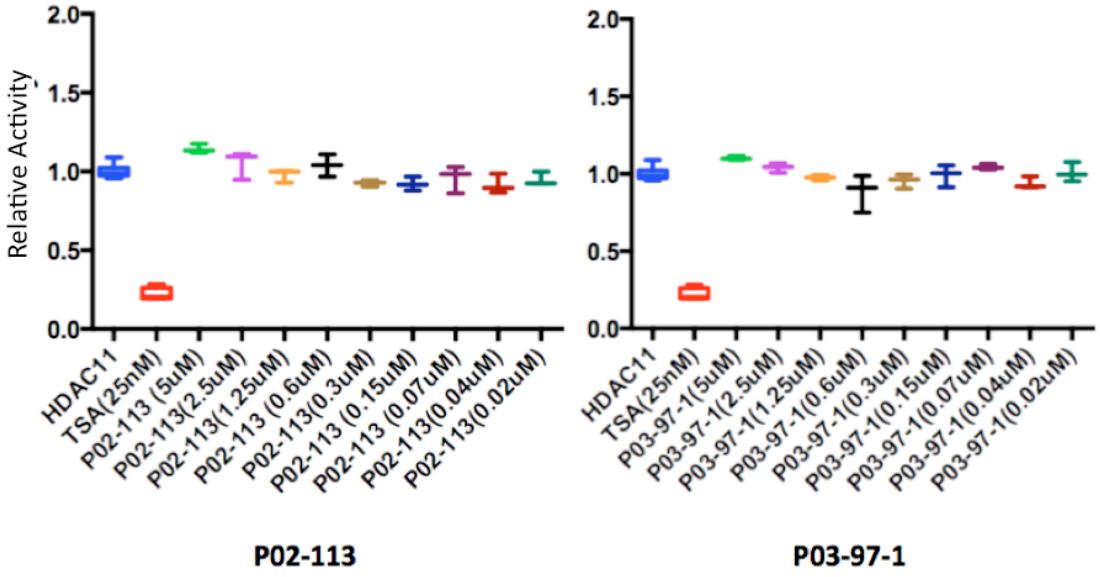

Figure 3.14 Class IV HDAC activity (HDAC11) was unaffected after treatment with P02-113 or P03-97-1. Mean activity with standard error of HDAC11 was measured upon treatment with P02-113 or P03-97-1 between the concentrations 5 µm to 0.02 µm with no significant change seen. HDAC11 activity was measured using the HDAC-Glo™ I/II Assay and Screening System (Promega).

4 Discussion

4.1 Immune response to TC-1 and A9 cell lines *in vivo*

The immune system is responsible for the recognition and elimination of cancerous cells. While both arms of the immune system, innate and adaptive, participate in this process the endogenous APP of the adaptive immune system is of particular importance. The endogenous APP allows the TCR present on the surface of CTLs to recognize MHC-I molecules present on the surface of all nucleated cells and determine if an adaptive immune response should be initiated. Due to the importance of this pathway in immune surveillance there seems to be a strong selective pressure for many cancers to down-regulate components involved in the endogenous APP (75-78). Of the different proteins involved, TAP-1 and MHC-I are the most frequently down regulated and can approach 100% reduction in some carcinomas (9-11, 23, 24).

Because the A9 metastatic cell line has reduced expression of both TAP-1 and MHC-I in comparison to its primary counterpart TC-1, I hypothesized that the immune response between the two cell lines would be significantly different *in vivo.* Upon analysis it was evident that the A9 cell line had a growth advantage over the TC-1 cell line in wild type mice. The A9 tumours became measurable 14 days after inoculation (Figure 3.3), almost twice as fast as the TC-1 tumours, which only became measurable at day 25 (Figure 3.2). The A9 tumours were also found to be significantly more aggressive as the mice had to be sacrificed at an earlier time point due to ulceration in several mice.

To further specify if the difference in tumour growth between the TC-1 and A9 cell lines is attributable to the endogenous APP, both cell lines were evaluated for tumour growth in mouse models lacking various components of the immune system. The models chosen were mice lacking CTLs ($CD8^{-/-}$) representing the endogenous APP, mice lacking T helper cells ($CD4^{-/-}$) representing the exogenous APP, and mice lacking eosinophils ($GATA1^{-/-}$) which are known to play a role in the elimination of some cancers.

As predicted, the TC-1 cell line had a significantly larger tumours (p-value < 0.0001) in mice lacking CTLs as compared to the wild type control (Figure 3.5). While the TC-1 cells retain the expression of TAP-1 and MHC-I, the mice lacking CTLs have

no immune cells to recognize the MHC-I molecules and therefore cannot initiate an appropriate immune response to tumours.

Interestingly, the mice without T helper cells representing the exogenous APP also showed a difference in tumour growth compared to wild type mice (p-value = 0.018), indicating that T helper cells also contribute in the reduction of TC-1 tumour burden. A possible explanation for this observation is that T helper cells are known to play a role in maintaining CTL activity after initial activation by cancer cells (79). Therefore, with no T helper cells present, CTL activity may be significantly reduced, resulting in faster tumour growth.

As for the mice lacking eosinophils, there was no significant change in tumour burden compared to the wild type mice, indicating these cells do not play a role in the recognition of the TC-1 cell line. This is consistent with recent studies showing that the role of eosinophils in cancer is largely dependent on the tumour type (81,82). Overall, it is clear from this experiment that the immune system is utilizing CTLs to detect and eliminate TC-1 cancer cells and that T helper cells may also be crucial in maintaining this response.

Furthermore the same *in vivo* experiment was performed using the A9 cell line with the hypothesis that there would be no significant difference in tumour growth between wild type and any of the knockout mice. As hypothesized I found no significant difference in tumours between wild type mice and mice lacking CTLs, T helper cells or eosinophils, however, mice lacking T helper cells had the most aggressive tumours (Figure 3.6). This may be attributed to their role in responding to professional antigen presenting cells that present exogenous peptides to the T helper cells through MHC-II in the tumour environment. However, to confirm the role of the immune cells evaluated a study longer than 20 days will be needed and will require innoculation of fewer A9 cells to prevent early termination due to ulceration. Future studies should also include other immune knockout models, such as natural killer cells and macrophages, to eliminate the role of other immune cells in recognition of both the TC-1 and A9 cell lines.

4.2 Therapeutic potential

Since it was discovered that the immune system plays an essential role in reducing the occurrence and severity of cancers, the field of cancer immunotherapy has significantly grown (83, 84). Cancer immunotherapy works by initiating an immune response against cancer cells. Currently there are several cancer immunotherapeutic agents in development, including biologicals such as monoclonal antibodies (mAbs), vaccines and cytokines as well as cellular therapies such as adoptive cellular therapy (ACT) (83, 84). Of these, mAbs have shown the greatest potential and are often targeted against immune cells, opposed to cancer cells, allowing them to treat a range of cancer types (83). The mAbs are often used to target programmed cell-death protein 1 (PD-1) or cytotoxic T-lymphocyte protein 4 (CTLA-4) both located on surface of T lymphocytes that function as inhibitory receptors involved in immune checkpoint signalling (83). By blocking either of these receptors, using mAbs, cancer cells are no longer able to inhibit T lymphocyte activation via their corresponding receptors. Alternatively to biologics, ACT works by *ex vivo* manipulation and expansion of T-lymphocytes to target cancer cells (83). There are currently several techniques under-development including the selection and expansion of tumour infiltrating lymphocytes (TILs), gene transfer of a synthetic TCR (sTCR) and the transfer of a chimeric antigen receptor (CAR) into T cells (83). While many of these therapies show great potential there are still a significant amount of patients that show no response (83,84). Of the patients experiencing no benefit it has been predicted that a percentage of the patient's remain unaffected due to deficiencies in the APM within their tumours (83). Therefore combination therapies may be key in the future, where the addition of drugs targeting the up regulation of the APM will be utilized (84).

While S-(+) curcuphenol has previously been shown by the Jefferies lab to up-regulate the APM, its synthesis and isolation is greatly hindered due to chirality (69). However this issue was overcome by the synthesis of curcuphenol analogues lacking chirality. The newly synthesized analogues were screened for the ability to up-regulate the APM in a murine metastatic lung carcinoma cell line, A9, *in vitro* and from this screen two analogues were selected: P02-113 and P03-97-1. Both P02-113 and P03-97-1 were futher evaluated in a tumour trial *in vivo* using the same A9 murine metastatic lung

carcinoma . Both compounds exhibited preventitive properties *in vivo*, as tumour growth was reduced in comparison to mice treated with the vehicle alone. However, P03-97-1 exhibited a stronger effect, which may be attributed stronger binding affinities to HDAC enzymes, or better ability to enter A9 cells, however the exact reason remains to be determined. Due to the stronger anti-cancer properties of P03-97-1 as well as increased stimulation of CTLs into tumours, P03-97-1 is a stronger candidate for future combination therapies where it could induce the expression of the MHC-I molecules and increase survival for patients whose cancers show an immune evasive phenotype due to reduced levels of the APM. However optimization of the dosing of P03-97-1 will be required as it was found to have a high rate of elimination from mouse plasma and becomes undetectable after six hours. Therefore to increase its therapeutic potential and gain a statistically significant difference in tumour burden *in vivo* an increase in dosing regimen may be required. Alternatively, a different route of administration, such as gavage, could allow for higher dosage concentrations without increasing the dosage regimen. Furthermore experimenting with the chemical structures of the compounds may also lead to more potent or soluble compounds that could increase therapeutic potential.

4.3 HDAC activity of P02-113 or P03-97-1

Due to the similar structure of the curcuphenol analogues to a known HDACi, TSA, which promotes the expression of MHC-I in the A9 cell line (9-11) it was predicted that the analogues were acting through a similar mechanism. However, upon a generalized class I/II HDAC luminescence assay to measure HDAC activity, using A9 cells, the opposite effect was discovered and HDAC activity was enhanced. Of the two compounds, P03-97-1 maintained peak levels of HDAC activity until the highest concentration of 1 uM suggesting a stronger effect, which may be attributed to stronger binding affinity to HDAC enzymes or reduced metabolism of the molecule, suggesting P03-97-1 is a better enhancement agent. Regardless of the potency exhibited by P02-113 and P03-97-1 in HDAC enhancement (HDACe) this is a completely novel activity that has never been seen in the literature for class I/II HDACs. However, there is one known HDAC activator for the class III HDACs, resveratrol, which indirectly acts upon SIRT1 (85). Therefore to determine if P02-113 and P03-97-1 were in fact directly interacting

with HDAC enzymes to promote activity, individual purified recombinant HDACs were assessed following treatment with the analogues. While the majority of HDAC enzymes did not show a change in activity, one enzyme, HDAC8, was inhibited by both P02-113 and P03-97-1. This is interesting as this is the only class I HDAC that is known to exist in both the nucleus and cytoplasm and diverged early in evolution from the other class I enzymes (86). This targeted inhibition of HDAC8 is a unique feature of the compounds as the majority of current HDAC inhibitors show pan HDACi. Therefore these analogues present a more targeted and optimal affinity then has been seen before. Luckily it is known that increased HDAC8 activity is associated with cancer as well as in other diseases including neurodegenerative disorders, metabolic deregulation, autoimmune and inflammatory diseases (86). Therefore these compounds could hold potential as specific HDAC8 inhibitors in the treatment of not only cancer but also other diseases. In regard to the APM it has been demonstrated that HDAC8 acts as a scaffold for cAMP responsive element binding protein (CREB), a known transcriptional up-regulator of TAP-1 and MHC-1 (83). One study showed upon over-expression of HDAC8, CREB phosphorylation became decreased along with its transcriptional activity (87). To determine if the increased expression of the APM is directly correlated with the inhibitory activity of P02-113 and P03-97-1 on HDAC8, further experiments in which HDAC8 is knocked down in the TC-1 cell line and APM expression is measured will be required. HDAC8 has previously been knocked-down using RNA interference in lung, colon and cervical cancer cell lines resulting in reduced proliferation while its over-expression in hepatocellular carcinoma promoted proliferation and inhibited apoptosis, however the APM remains to be examined (88, 89).

Alternatively to HDACi there were two HDACs, 5 and 10, which showed an enhanced activity upon treatment with P02-113 and P03-97-1. These are most likely the HDAC candidates showing an increase in activity in the generalized HDAC class I/II assay preformed on the A9 cell line. This is a unique finding as HDACs are currently viewed as being overactive in cancers and decrease the expression of cancer-preventing genes. However, reductions in activity of both HDACs 5 and 10 have been implemented in advanced stages of lung cancer and are correlated with poor outcome (90, 91). Interestingly previous studies that have down regulated HDAC5 using siRNA found that

there was a pro-angiogenic effect due to increased endothelial cell migration, sprouting, and tube formation (92). As for HDAC10, there is significantly more research in relation to its activity in cancer. Decreases in HDAC10 activity have been correlated with more aggressive malignancies in B cell and gastric cancers and have been correlated with metastasis in gastric cancer and squamous cell carcinomas (93-95). A mechanism has also been proposed for the involvement of HDAC10 in metastasis, as it is known to suppress matrix metalloproteases 2 and 9 that are critical for cancer cell invasion and metastasis (93). Future work to establish if HDAC5 and HDAC10 are crucial to the up-regulation of the APM will be fundamental to understand if P02-113 and P03-97-1 exhibit this function through the enhancement of HDACs 5 and 10. Down-regulation of these enzymes in the primary TC-1 cell lines will help establish if this is a contributing mechanism.

Bibliography

1. Laird, P. W., & Jaenisch, R. The role of DNA methylation in cancer genetics and epigenetics. *Annual review of genetics* **30**(1), 441-464 (1996).
2. Bishop, J. M. The molecular genetics of cancer. *Science* **235**(4786), 305-311 (1987).
3. Nguyen, D. X., & Massagué, J. Genetic determinants of cancer metastasis. *Nature Reviews Genetics* **8**(5), 341-352 (2007).
4. Jones, P. A., & Baylin, S. B. The fundamental role of epigenetic events in cancer. *Nature reviews genetics* **3**(6), 415-428 (2002).
5. Balmain, A., Gray, J., & Ponder, B. The genetics and genomics of cancer. *Nature genetics* **33**, 238-244 (2003).
6. Esteller, M. Epigenetics in cancer. *New England Journal of Medicine* **358**(11), 1148-1159 (2008).
7. Escors, D. Tumour immunogenicity, antigen presentation, and immunological barriers in cancer immunotherapy. *New journal of science* (2014).
8. Seliger, B., Cabrera, T., Garrido, F. & Ferrone, S. HLA class I antigen abnormalities and immune escape by malignant cells. *Semin Cancer Biol* **12**, 3-13 (2002).
9. Setiadi, A.F., Omilusik, K., David, M.D., Seipp, R.P., Hartikainen, J., Gopaul, R., Choi, K.B. & Jefferies, W.A. Epigenetic enhancement of antigen processing and presentation promotes immune recognition of tumors. *Cancer research* **68**(23) 9601-9607 (2008).
10. Setiadi, A. F., David, M. D., Seipp, R. P., Hartikainen, J. A., Gopaul, R., & Jefferies, W. A. Epigenetic control of the immune escape mechanisms in malignant carcinomas. *Molecular and cellular biology **27***(22), 7886-7894 (2007).
11. Setiadi, A. F., David, M. D., Chen, S. S., Hiscott, J., & Jefferies, W. A. Identification of mechanisms underlying transporter associated with antigen processing deficiency in metastatic murine carcinomas. *Cancer research* **65**(16), 7485-7492 (2005).
12. 2016. Cancer statistics at a glance. *Canadian Cancer Society.*
13. Tomlinson, I., & Bodmer, W. Selection, the mutation rate and cancer: ensuring that the tail does not wag the dog. *Nature medicine* **5**(1), (1999).
14. Mehlen, P., & Puisieux, A. Metastasis: a question of life or death. *Nature Reviews Cancer* **6**(6), 449-458 (2006).

15. Overveiw of Metastasis. Cancerquest (2016).
16. Nguyen, D. X., & Massagué, J. Genetic determinants of cancer metastasis. *Nature Reviews Genetics* **8**(5), 341-352 (2007).
17. Jones, P. A., & Baylin, S. B. The fundamental role of epigenetic events in cancer. *Nature reviews genetics* **3**(6), 415-428 (2002).
18. Kim, R., Emi, M., & Tanabe, K. Cancer immunoediting from immune surveillance to immune escape. *Immunology* **121**(1), 1-14(2007).
19. Reiman, J. M., Kmieciak, M., Manjili, M. H., & Knutson, K. L. Tumor immunoediting and immunosculpting pathways to cancer progression. *Seminars in cancer biology* **17**(4), 275-287 (2007).
20. Thompson, A. E. The immune system. *Jama* **313**(16), 1686-1686 (2015).
21. Shreffler, D. C., & David, C. S. The H-2 major histocompatibility complex and the/immune response region: genetic variation, function, and organization. *Advances in immunology* **20**, 125-195 (1975).
22. Cromme F.V., Van Bommel P.F., Walboomers J.M., Gallee M.P., Stern P.L., Kenemans P., Helmerhorst T.J., Stukart M.J., & Meijer C.J. Differences in MHC and TAP-1 expression in cervical cancer lymph node metastases as compared with the primary tumours. *British journal of cancer* 69(6), 1176 (1994).
23. Cabrera, T., Salinero, J., Fernandez, M. A., Garrido, A., Esquivias, J., & Garrido, F. High frequency of altered HLA class I phenotypes in laryngeal carcinomas. *Hum Immunol* **61**, 499-506 (2000).
24. Seliger, B., Maeurer, M. J., & Ferrone, S. Antigen-processing machinery breakdown and tumor growth. *Immunology today* **21**(9), 455-464 (2000).
25. Garcia‐Lora, A., Algarra, I., & Garrido, F. MHC class I antigens, immune surveillance, and tumor immune escape. *Journal of cellular physiology* **195**(3), 346-355 (2003).
26. Seliger, B., Höhne, A., Knuth, A., Bernhard, H., Meyer, T., Tampe, R., Momburg, F., & Huber, C. Analysis of the major histocompatibility complex class I antigen presentation machinery in normal and malignant renal cells: evidence for deficiencies associated with transformation and progression. *Cancer research* **56**(8), 1756-1760 (1996).

27. Cromme, F. V., Van Bommel, P. F., Walboomers, J. M., Gallee, M. P., Stern, P. L., Kenemans, P., Helmerhorst, T. J., Stukart, M. J., & Meijer, C. J. Differences in MHC and TAP-1 expression in cervical cancer lymph node metastases as compared with the primary tumours. *British journal of cancer* **69**(6), 1176 (1994).
28. Johnsen, A., France, J., Sy, M. S., & Harding, C. V. Down-regulation of the transporter for antigen presentation, proteasome subunits, and class I major histocompatibility complex in tumor cell lines. *Cancer research* **58**(16), 3660-3667 (1998).
29. Concha-Benavente, F., Srivastava, R., Ferrone, S., & Ferris, R. L. Immunological and clinical significance of HLA class I antigen processing machinery component defects in malignant cells. *Oral Oncology* (2016).
30. Visser, K. E., Eichten, A., & Coussens, L. M. Paradoxical roles of the immune system during cancer development. *Nature reviews cancer* **6**(1), 24-37 (2006).
31. Schnare, M., Barton, G. M., Holt, A. C., Takeda, K., Akira, S., & Medzhitov, R. Toll-like receptors control activation of adaptive immune responses. *Nature immunology* **2**(10), 947-950 (2001).
32. Iwasaki, A., & Medzhitov, R. Regulation of adaptive immunity by the innate immune system. *Science* **327**(5963), 291-295 (2010).
33. Roche, P. A., & Furuta, K. The ins and outs of MHC class II-mediated antigen processing and presentation. *Nature Reviews Immunology* **15**(4), 203-216 (2015).
34. Rock, K. L., & Goldberg, A. L. Degradation of cell proteins and the generation of MHC class I-presented peptides. *Annual review of immunology* **17**(1), 739-779 (1999).
35. Agrawal, S., & Kishore, M.C. MHC class I gene expression and regulation. *Journal of hematotherapy & stem cell research* **9.6**, 795-812 (2000).
36. Vigushin, D. M., Ali, S., Pace, P. E., Mirsaidi, N., Ito, K., Adcock, I., & Coombes, R. C. Trichostatin A is a histone deacetylase inhibitor with potent antitumor activity against breast cancer in vivo. *Clinical Cancer Research* **7**(4), 971-976 (2001).
37. Feinberg, A. P., & Vogelstein, B. Hypomethylation distinguishes genes of some human cancers from their normal counterparts. *Nature* **301**(5895), 89-92 (1983).

38. Cock‐Rada, A., & Weitzman, J. B. The methylation landscape of tumour metastasis. *Biology of the Cell* **105**(2), 73-90 (2013).
39. Campoli, M., & Ferrone, S. HLA antigen changes in malignant cells: epigenetic mechanisms and biologic significance. *Oncogene* **27**(45), 5869-5885 (2008).
40. Dawson, M. A., & Kouzarides, T.Cancer epigenetics: from mechanism to therapy. *Cell* **150**(1), 12-27 (2012).
41. Ma, X., Ezzeldin, H. H., & Diasio, R. B. Histone Deacetylase Inhibitors. *Drugs* **69**(14), 1911-1934 (2009).
42. Kroesen, M., Gielen, P., Brok, I. C., Armandari, I., Hoogerbrugge, P. M., & Adema, G. J. HDAC inhibitors and immunotherapy; a double edged sword. *Oncotarget* **5**(16), 6558-72, (2014).
43. Rodríguez-Paredes, M., & Esteller, M. Cancer epigenetics reaches mainstream oncology. *Nature medicine*, 330-339 (2011).
44. Lai, P. K., & Roy, J. Antimicrobial and chemopreventive properties of herbs and spices. *Current medicinal chemistry* **11**(11), 1451-1460 (2004).
45. Thompson, L. U., Rickard, S. E., Orcheson, L. J., & Seidl, M. M. Flaxseed and its lignan and oil components reduce mammary tumor growth at a late stage of carcinogenesis. *Carcinogenesis* **17**(6), 1373-1376 (1996).
46. Abdullaev, F. I. Cancer chemopreventive and tumoricidal properties of saffron (Crocus sativus L.). *Experimental biology and medicine* **227**(1), 20-25 (2002).
47. Busquets, S., Carbó, N., Almendro, V., Quiles, M. T., López-Soriano, F. J., & Argilés, J. M. Curcumin, a natural product present in turmeric, decreases tumor growth but does not behave as an anticachectic compound in a rat model. *Cancer letters* **167**(1), 33-38 (2001).
48. Greenwell, M., & Rahman, P. K. S. M. Medicinal Plants: Their Use in Anticancer Treatment. *International journal of pharmaceutical sciences and research* **6**(10), 4103 (2015).
49. Simmons, T. L., Andrianasolo, E., McPhail, K., Flatt, P., & Gerwick, W. H. Marine natural products as anticancer drugs. *Molecular Cancer Therapeutics* **4**(2), 333-342 (2005).

50. Gomes, N. G., Dasari, R., Chandra, S., Kiss, R., & Kornienko, A. Marine Invertebrate Metabolites with Anticancer Activities: Solutions to the "Supply Problem". *Marine drugs* **14**(5), 98 (2016).
51. Rodrigo, G., Almanza, G. R., Cheng, Y., Peng, J., Hamann, M., Duan, R. D., & Åkesson, B. Antiproliferative effects of curcuphenol, a sesquiterpene phenol. *Fitoterapia* **81**(7), 762-76 (2010).
52. Gaspar, H., Feio, S. S., Rodrigues, A. I., & Van Soest, R. Antifungal activity of (+)-curcuphenol, a metabolite from the marine sponge didiscus oxeata. *Marine Drugs* **2**(1), 8-13 (2004).
53. El Sayed, K. A., Yousaf, M., Hamann, M. T., Avery, M. A., Kelly, M., & Wipf, P. Microbial and Chemical Transformation Studies of the Bioactive Marine Sesquiterpenes (S)-(+)-Curcuphenol and-Curcudiol Isolated from a Deep Reef Collection of the Jamaican Sponge Didiscus o xeata. *Journal of natural products* **65**(11), 1547-1553 (2002).
54. Behery, F. A., Sallam, A. A., & El Sayed, K. AMannich-and Lederer–Manasse-based analogues of the natural product S-(+)-curcuphenol as cancer proliferation and migration inhibitors. *Med Chem Comm* **3**(10), 1309-1315 (2012).
55. Fusetani, N., Sugano, M., Matsunaga, S., & Hashimoto, K. (+)-curcuphenol and dehydrocurcuphenol, novel sesquiterpenes which inhibit H, K-ATPase, from a marine sponge Epipolasis sp. *Cellular and Molecular Life Sciences* **43**(11), 1234-1235 (1987).
56. Wright, A. E., Pomponi, S. A., McConnell, O. J., Kohmoto, S., & McCarthy, P. J. (+)-Curcuphenol and (+)-Curcudiol, Sesquiterpene Phenols from Shallow and Deep Water Collections of the Marine Sponge Didiscus flavus. *Journal of Natural Products* **50**(5), 976-978 (1987).
57. Behery, F. A., Sallam, A. A., & El Sayed, K. A. Mannich-and Lederer–Manasse-based analogues of the natural product S-(+)-curcuphenol as cancer proliferation and migration inhibitors. *MedChemComm* **3**(10), 1309-1315 (2012).
58. Gaspar, H., Moiteiro, C., Sardinha, J., & González-Coloma, A. Bioactive Semisynthetic Dervatives of (S)-(+)-Curcuphenol (2008).

59. Cichewicz, R.H., Clifford, L.J., Lassen, P.R., Cao, X., Freedman, T.B., Nafie, L.A., Deschamps, J.D., Kenyon, V.A., Flanary, J.R., Holman, T.R. & Crews, P. Stereochemical determination and bioactivity assessment of (S)-(+)-curcuphenol dimers isolated from the marine sponge Didiscus aceratus and synthesized through laccase biocatalysis. *Bioorganic & medicinal chemistry* **13** (19), 5600-5612 (2005).
60. Tsukamoto, S., Kato, H., Hirota, H., & Fusetani, N. Antifouling terpenes and steroids against barnacle larvae from marine sponges 283-291 (1997).
61. Chung, H.M., Hong, P.H., Su, J.H., Hwang, T.L., Lu, M.C., Fang, L.S., Wu, Y.C., Li, J.J., Chen, J.J., Wang, W.H. & Sung, P.J. Bioactive compounds from a gorgonian coral Echinomuricea sp. (Plexauridae). *Marine drugs* **10**(5), 1169-1179 (2012).
62. Takamatsu, S., Hodges, T. W., Rajbhandari, I., Gerwick, W. H., Hamann, M. T., & Nagle, D. G. Marine natural products as novel antioxidant prototypes. *Journal of Natural Products* **66**(5), 605-608 (2003).
63. Hertiani, T., Edrada-Ebel, R. A., & Kubbutat, M. Protein kinase inhibitors from Indonesian Sponge Axynissa sp. Indonesian Journal of Pharmacy 78-85 (2008).
64. Frame, M. C. Src in cancer: deregulation and consequences for cell behaviour. *Biochimica et Biophysica Acta (BBA)-Reviews on Cancer* **1602**(2), 114-130 (2002).
65. Valdivia, A. C., Boketof, Å., Olde, B., Owman, C., Vilaseca, A., Fuentes, L., & Sterner, O. Activation of the free fatty acid receptor GPR40 by (+)-curcuphenol and related synthetic compounds. *Revista Boliviana de Química* **26**(2), 77-82 (2009).
66. Yonezawa, T., Katoh, K., & Obara, Y. Existence of GPR40 functioning in a human breast cancer cell line, MCF-7. *Biochemical and biophysical research communications* **314**(3), 805-809 (2004).
67. Hardy, S., St-Onge, G. G., Joly, É., Langelier, Y., & Prentki, M. Oleate promotes the proliferation of breast cancer cells via the G protein-coupled receptor GPR40. *Journal of Biological Chemistry* **280**(14), 13285-13291(2005).
68. Tomita, T., Masuzaki, H., Iwakura, H., Fujikura, J., Noguchi, M., Tanaka, T. & Fujimoto, K. Expression of the gene for a membrane-bound fatty acid receptor in the pancreas and islet cell tumours in humans: evidence for GPR40 expression in

pancreatic beta cells and implications for insulin secretion. *Diabetologia* **49**(5), 962-968 (2006).

69. Creier, C. *Investigation of extract influence on antigen presentation in Nef-expressing dendritic cells and cancer cells.* MS thesis. University of Applied Sciences Mannheim (2011).
70. Chung, H.M., Hong, P.H., Su, J.H., Hwang, T.L., Lu, M.C., Fang, L.S., Wu, Y.C., Li, J.J., Chen, J.J., Wang, W.H. & Sung, P.J. Bioactive compounds from a gorgonian coral Echinomuricea sp.(Plexauridae). *Marine drugs **10***(5), 1169-1179 (2012).
71. Chen, C. Y., Shen, Y. C., Chen, Y. J., Sheu, J. H., & Duh, C. Y. Bioactive sesquiterpenes from a Taiwanese marine sponge Parahigginsia sp. *Journal of natural products* **62**(4), 573-576 (1999).
72. Šmahel, M., Šıma, P., Ludvıková, V., Marinov, I., Pokorná, D., & Vonka, V. Immunisation with modified HPV16 E7 genes against mouse oncogenic TC-1 cell sublines with downregulated expression of MHC class I molecules *Vaccine* **21**(11), 1125-1136 (2003).
73. Yu, C., Cantor, A. B., Yang, H., Browne, C., Wells, R. A., Fujiwara, Y., & Orkin, S. H. Targeted deletion of a high-affinity GATA-binding site in the GATA-1 promoter leads to selective loss of the eosinophil lineage in vivo. *The Journal of experimental medicine* **195**(11), 1387-1395 (2002).
74. Sanderson, L., Taylor, G. W., Aboagye, E. O., Alao, J. P., Latigo, J. R., Coombes, R. C., & Vigushin, D. M. Plasma pharmacokinetics and metabolism of the histone deacetylase inhibitor trichostatin a after intraperitoneal administration to mice. *Drug Metabolism and Disposition* **32**(10), 1132-1138 (2004).
75. Manning, J., Indrova, M., Lubyova, B., Pribylova, H., Bieblova, J., Hejnar, J., Simova, J., Jandlova, T., Bubenik, J., & Reinis, M. Induction of MHC class I molecule cell surface expression and epigenetic activation of antigen‐processing machinery components in a murine model for human papilloma virus 16‐associated tumours. *Immunology* **123**(2), 218-227(2008).
76. Indrová, M., Bieblová, J., Jandlová, T., Vonka, V., Pajtasz-Piasecka, E., & Reinis, M. Chemotherapy, IL-12 gene therapy and combined adjuvant therapy of HPV 16-

associated MHC class I-proficient and-deficient tumours. *International journal of oncology* **28**(1), 253 (2006).

77. Cromme, F. V., Airey, J., Heemels, M. T., Ploegh, H.L., Keating, P.J., Stern, P.L., Meijer, C.J. & Walboomers, J.M. Loss of transporter protein, encoded by the TAP-1 gene, is highly correlated with loss of HLA expression in cervical carcinomas. *The Journal of experimental medicine* **179**(1) 335-340 (1994).
78. Maeurer, M.J., Gollin, S.M., Martin, D., Swaney, W., Bryant, J., Castelli, C., Robbins, P., Parmiani, G., Storkus, W.J., &. Lotze, M.T. Tumor escape from immune recognition: lethal recurrent melanoma in a patient associated with downregulation of the peptide transporter protein TAP-1 and loss of expression of the immunodominant MART-1/Melan-A antigen. *Journal of Clinical Investigation* 98 (7), 1233 (1996).
79. Huang, H., Hao, S., Li, F., Ye, Z., Yang, J., & Xiang, J. CD4+ Th1 cells promote CD8+ Tc1 cell survival, memory response, tumor localization and therapy by targeted delivery of interleukin 2 via acquired pMHC I complexes. *Immunology* **120**(2), 148-159 (2007).
80. Sakkal, S., Miller, S., Apostolopoulos, V., & Nurgali, K. Eosinophils in Cancer: Favourable or Unfavourable?. *Current medicinal chemistry*, **23**(7), 650-666 (2016).
81. Venkatesan, R., Salam, A., Alawin, I., & Willis, M. Non-small cell lung cancer and elevated eosinophil count: A case report and literature review. *Cancer Treatment Communications* **4**, 55-58 (2015).
82. Astigiano, S., Morandi, B., Costa, R., Mastracci, L., D'Agostino, A., Battista Ratto, G., Melioli, G., & Frumento, G. Eosinophil granulocytes account for indoleamine 2, 3-dioxygenase-mediated immune escape in human non small cell lung cancer.*Neoplasia* **7**(4), 390-396 (2005).
83. Khalil, D. N., Smith, E. L., Brentjens, R. J., & Wolchok, J. D. The future of cancer treatment: immunomodulation, CARs and combination immunotherapy. *Nature Reviews Clinical Oncology* **13**(5), 273-290 (2016).
84. Abken, H., Chmielewski, M., & Hombach, A. A. Antigen-specific T-cell activation independently of the MHC: chimeric antigen receptor-redirected T cells. *Frontiers in immunology* **4**, 371 (2013).

85. Beher, D., Wu, J., Cumine, S., Kim, K. W., Lu, S. C., Atangan, L., & Wang, M. Resveratrol is not a direct activator of SIRT1 enzyme activity. *Chemical biology & drug design* **74**(6), 619-624 (2009).
86. Chakrabarti, A., Oehme, I., Witt, O., Oliveira, G., Sippl, W., Romier, C., Pierce, R.J. & Jung, M. HDAC8: a multifaceted target for therapeutic interventions. *Trends in pharmacological sciences* **36**(7), 481-492 (2015).
87. Gao, J., Siddoway, B., Huang, Q., & Xia, H. Inactivation of CREB mediated gene transcription by HDAC8 bound protein phosphatase. *Biochemical and biophysical research communications* **379**(1), 1-5 (2009).
88. Wu, J., Du, C. Lv, Z., Ding, C., Cheng, J., Xie, H., Zhou, L., & Zheng, S.The up-regulation of histone deacetylase 8 promotes proliferation and inhibits apoptosis in hepatocellular carcinoma. *Digestive diseases and sciences* **58** (12), 3545-3553 (2013).
89. Vannini, A., Volpari, C., Filocamo, G., Casavola, E.C., Brunetti, M., Renzoni, D., Chakravarty, P., Paolini, C., De Francesco, R., Gallinari, P., & Steinkühler, C. Crystal structure of a eukaryotic zinc-dependent histone deacetylase, human HDAC8, complexed with a hydroxamic acid inhibitor. *Proceedings of the National Academy of Sciences of the United States of America* **101**(42), 15064-15069 (2004).
90. Yao, H., & Rahman, I. Current concepts on the role of inflammation in COPD and lung cancer. *Current opinion in pharmacology* **9**(4), 375-383 (2009).
91. Osada, H., Tatematsu, Y., Saito, H., Yatabe, Y., Mitsudomi, T., & Takahashi, T. Reduced expression of class II histone deacetylase genes is associated with poor prognosis in lung cancer patients. *International journal of cancer* **112**(1), 26-32(2004).
92. Urbich, C., Rössig, L., Kaluza, D., Potente, M., Boeckel, J.N., Knau, A., Diehl, F., Geng, J.G., Hofmann, W.K., Zeiher, A.M. & Dimmeler, S. HDAC5 is a repressor of angiogenesis and determines the angiogenic gene expression pattern of endothelial cells. *Blood* **113(**22), 5669-5679 (2009).
93. Song, C., Zhu, S., Wu, C., & Kang, J. Histone deacetylase (HDAC) 10 suppresses cervical cancer metastasis through inhibition of matrix metalloproteinase (MMP) 2 and 9 expression. *Journal of Biological Chemistry* **288**(39), 28021-28033(2013).

94. Jin, Z., Jiang, W., Jiao, F., Guo, Z., Hu, H., Wang, L., & Wang, L. Decreased expression of histone deacetylase 10 predicts poor prognosis of gastric cancer patients. *Int J Clin Exp Pathol* **7**(9), 5872-5879(2014).
95. Powers, J., Lienlaf, M., Perez-Villarroel, P., Deng, S., Knox, T., Villagra, A., & Sahakian, E. Expression and Function of Histone Deacetylase 10 (HDAC10) in B Cell Malignancies. *Histone Deacetylases: Methods and Protocols* 129-145(2016).